Electromagnetic leptonic decays and structure of light mesons

L. G. Landsberg

Institute of High-Energy Physics, Serpukhov

Usp. Fiz. Nauk **146**, 185–236 (June 1985)

Recent experimental and theoretical data on the rare electromagnetic conversion decays of light mesons ($A\to B\gamma_v\to Bl^+l^-$) are reviewed. In these decays, the photon is a virtual photon (γ_v) and converts into a lepton pair l^+l^-. Study of the effective-mass spectrum of the lepton pairs reveals the dynamic transition form factor F_{AB} ($q^2=m^2_{l^+l^-}$), which characterizes the electromagnetic structure of the A→B transition vertex. Such studies have been undertaken for the decays $\pi^0\to e^+e^-\gamma$, $\eta\to\mu^+\mu^-\gamma$, $\eta'\to\mu^+\mu^-\gamma$, $\omega\to\pi^0\mu^+\mu^-$, and several similar processes. Analysis of the results reveals that the general behavior of the transition form factors of the neutral mesons agrees with vector dominance and with various versions of the quark model. There are, on the other hand, some quantitative deviations from vector dominance in the decays $\pi^0\to e^+e^-\gamma$ and $\omega\to\pi^0\mu^+\mu^-$. Data on the electromagnetic leptonic processes of higher orders, such as the decays $\eta\to\mu^+\mu^-$ and $\pi^0\to e^+e^-$, and their relationship with the structure of mesons are discussed. Various experimental searches are also discussed. The future outlook for such research is assessed.

TABLE OF CONTENTS

1. INTRODUCTION

Research on the electromagnetic decays of hadronic states is of considerable interest for reaching an understanding of the structure of hadronic matter and for learning about the fundamental mechanisms for the interactions of photons and hadrons. These electromagnetic processes are simpler and more amenable to a complete theoretical interpretation than purely hadronic interactions. They have accordingly become a proving ground for any theory describing the structure of strongly interacting particles.

Many of the questions which arise in an analysis of the electromagnetic decays of the "light" mesons (i.e., the particles consisting of the light u-, d-, and s-quarks and the corresponding antiquarks) were formulated a long time ago and already have a 15- or 20-year history. In recent years a new situation has developed in hadron physics because of the impressive successes of the theory of strong interactions—quantum chromodynamics (see Ref. 1, for example). Unfortunately, these new theoretical ideas have not yet been applied in a systematic way to the decays of light mesons, where the region of small momentum transfer and large range is very important. Apparently, we can expect genuine, really significant progress here only after we have acquired the theoretical tools for working at distances of the order of the confinement radius. Nevertheless, in those problems in which it is necessary to consider states with a large momentum transfer, e.g. in an analysis of the applicability of the vector dominance model (VDM) or in an evaluation of the amplitude for the decay of pseudoscalar mesons into a lepton pair, quantum chromodynamics (QCD) plays a very constructive role.

No matter how surprising it might seem at first glance, even these old questions went for a long time without more or less clear experimental answers. The results of many experiments have directly contradicted each other and have not made it possible to draw a common picture of electromagnetic hadronic phenomena. For example, the set of data on the radiative decays of vector and pseudoscalar mesons could not be explained at all without appealing to improbable hypotheses such as a strong breaking of isotopic invariance, an unusual structure for the electromagnetic current, or the existence of large anomalous magnetic moments of the quarks. The data obtained on the internal electromagnetic structure of neutral π^0 and η mesons from research on their conversion decays qualitatively and starkly contradict the

 0038-5670/85/060435-32$01.80

vector dominance model. Finally, the experimental results on the widths of several electromagnetic decays, such as $\eta \to \mu^+\mu^-$ and $\eta \to \pi^0\gamma\gamma$, disagree substantially with theoretical predictions.

The situation which developed was due primarily to the difficulty in studying experimentally electromagnetic decays of hadrons. These are usually rare processes, with low branching ratios. Their study requires high-luminosity experiments with a high intensity and the simultaneous detection of all the secondary decay particles (both charged particles and γ rays) for a reliable suppression of the numerous background processes. Only recently have developments in experimental apparatus made such experiments possible. In addition, important information on the electromagnetic widths of certain hadronic decays has been extracted from such subtle phenomena as the production of particles in a nuclear Coulomb field (the "Primakoff effect") or in $\gamma\gamma$ collisions. In the former case, reliable identification of Coulomb processes required experiments with a very large initial energy of the π and K mesons; in the latter case, experiments had to be carried out in colliding e^+e^- beams of high energy and high luminosity. It was only comparatively recently that all this became possible.

The experimental picture here has changed significantly over the past few years. It has been in the past few years that a thorough study of many electromagnetic properties of light mesons has been undertaken, and new and extremely interesting information has been obtained.

Recent experiments on the radiative decays of mesons have substantially extended our understanding of these processes. The results of new measurements of the corresponding radiative widths of vector (V) and pseudoscalar (P) mesons agree reasonably well with the predictions of the simple quark model. According to this model, the decays

$$V \to P + \gamma, \tag{1.1}$$

$$P \to V + \gamma \tag{1.2}$$

are magnetic dipole transitions, and their radiative widths can be expressed in terms of the magnetic moments of quarks under the assumption of SU(3) symmetry and a nonet symmetry, according to which the spatial wave functions of all the $q\bar{q}$ states with identical orbital quantum numbers are identical in form. The old experimental data, which did not fit into this picture at all, were found to be erroneous. The results of measurements of two-photon decays of pseudoscalar mesons,

$$P \to 2\gamma, \tag{1.3}$$

are also consistent with the quark model.

For a systematic and more comprehensive analysis of radiative decays (1.1), (1.2), and (1.3) it is necessary to incorporate relativistic effects; the breaking of SU(3) symmetry, the OZI rule, and vector dominance; and the breaking of the nonet symmetry. It is also necessary to introduce overlap integrals describing the overlap of the radial wave functions of the initial and final states, anomalous magnetic moments of the quarks, etc. However, such a detailed analysis would hardly be justified at this point since it would require data on the radiative widths which are much more accurate than the data presently available. Clearly, this circumstance should motivate further experiments in this important and promising field.

Research on the radiative decays of other mesons (axial, tensor, etc.) is still in a formative stage, and it is too early to try to draw a clear picture. A theoretical analysis of these decays is complicated by the circumstance that the analysis cannot be restricted to magnetic dipole transitions alone.

A discussion of the experimental and theoretical questions related to the radiative decays goes beyond the scope of the present review. To some extent, the corresponding material is given in some recent reviews and rapporteur talks,[2-6] along with an extensive bibliography.

The present review focuses on research on rare electromagnetic leptonic decays and on the use of these processes to study the electromagnetic structure of light neutral mesons.

Let us briefly review the situation involving the electromagnetic form factors of the elementary particles. One usually speaks in terms of charge and magnetic form factors, which characterize the spatial distribution of charges or magnetic moments of hadrons. Electromagnetic form factors are manifested in single-photon processes (ep, en, $\pi^\pm$ e, and $K^\pm$ e scattering) and also in the annihilation of an e^+e^- pair accompanied by the formation of a particle and an antiparticle $e^+e^- \to p\bar{p}$, $e^+e^- \to \pi^+\pi^-$, and $e^+e^- \to K^+K^-$. In all these experiments, the hadrons are, in a sense, probed by virtual photons in the region of spacelike momentum transfer in scattering processes or timelike momentum transfer in annihilation processes (Fig. 1). This probing can reveal the hadron form factors $E(q^2)$, which characterize the spatial distribution of the electric charge or magnetization of the hadrons. The spatial region which is studied is related to q^2 by $r^2 \sim 1/|q^2|$.

For neutral mesons M_0, single-photon exchange pro-

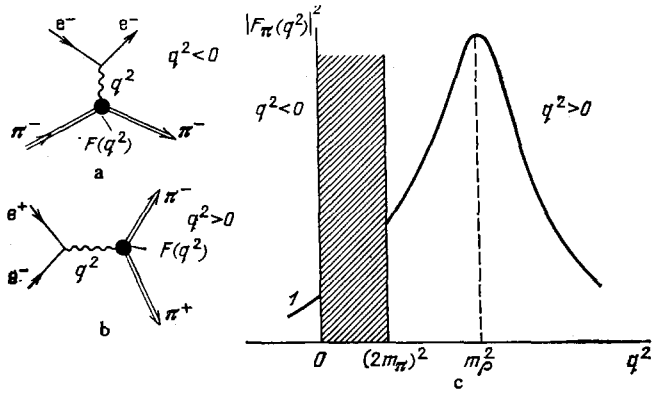

FIG. 1. The form factor of the π meson. a—Feynman diagram for π^-e scattering {the process occurs because of the exchange of a single virtual photon with a spacelike 4-momentum $q^2 < 0$ [the spatial structure of the hadron, i.e., its form factor $F_{\pi^-}(q^2)$, changes the cross section for the electromagnetic scattering: $(d\sigma/dq^2)_{\pi^-e} = (d\sigma/dq^2)_{point}[F_{\pi^-}(q^2)]^2$}; b—Feynman diagram for $e^+e^- \to \pi^+\pi^-$ annihilation [the process results from the exchange of a single virtual photon with a timelike 4-momentum $q^2 = s > 0$; the form factor for the π meson changes the annihilation cross section: $\sigma(s)e^+e^- \to \pi^+\pi^- = \sigma(s)_{point}|F_\pi(q^2)|^2$]; c—qualitative behavior of $|F_\pi(q^2)|^2$ over the entire q^2 range (the hatching shows the nonphysical region).

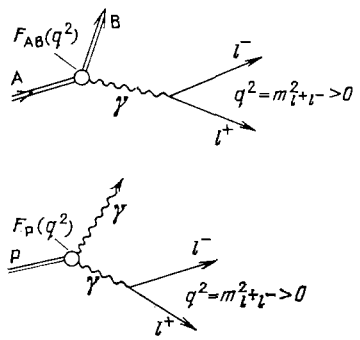

FIG. 2. Transition form factors of neutral mesons in conversion decays. The diagrams correspond to the decays $A\to Bl^+l^-$ and $P\to l^+l^-\gamma$. The transition form factor changes the spectrum of the lepton pairs: $(d\Gamma/dq^2)_{A\to Bl^+l^-} = (d\Gamma/dq^2)_{point}|F_{AB}(q^2)|^2$.

cesses are forbidden by the conservation of charge parity in electromagnetic interactions (we recall that truly neutral particles M_0 are characterized by a definite charge parity, while the charge parity of the photon is negative). Since the amplitudes of such single-photon processes are proportional to the electromagnetic form factors of the neutral mesons, $F(q^2)_{M_0}$, these electromagnetic form factors are always zero.

However, the complex internal structure of neutral hadrons may also be manifested in interactions in which a neutral particle with one charge parity converts into another particle with the opposite value of this quantum number.

Let us consider, for example, the electromagnetic radiative decay

$$A\to B+\gamma_\gamma \tag{1.4}$$

where A and B are the primary and secondary neutral mesons, with charge parities C_A and C_B; for the γ ray we have $C_\gamma = -1$. Since charge parity is conserved, we have $C_A = C_B C_\gamma = -C_B$; i.e., C_A and C_B must have opposite signs. If the radiative decay $A\to B+\gamma$ can occur, there is the further possibility of another process, in which the emitted γ ray "descends from the mass shell," becomes virtual, and then converts into a lepton pair:

$$A\to B+\gamma_V = B+l^++l^- \tag{1.5}$$

(Fig. 2). This phenomenon is called the "internal conversion" of the γ ray, while the decays $A\to B+l^++l^-$ are "conversion decays." For a conversion decay the probability for the production of a lepton pair with a definite effective mass $q^2=m^2_{l^+l^-}$ is proportional to the probability for the emission of a virtual γ ray with a timelike 4-momentum $q^2=m^2_{l^+l^-}$. The probability for the emission of such a photon, however, is determined by the electromagnetic structure of the region in which the transition of particles A and B occurs. In terms of Feynman diagrams we would say that the emission of virtual photons results from a dynamic electromagnetic structure which arises at the "vertex" of the transition $A\to B$ (Fig. 2). This electromagnetic structure, a consequence of the cloud of virtual states in the vicinity of the transition $A\to B$, is characterized by a distinctive form factor: the "transition form factor." For neutral hadrons, the ordinary ("static") form factors therefore vanish, but transition ("dynamic") form factors may arise because of the electromagnetic structure of the transition vertex.

Data on the electromagnetic structure of neutral A and B mesons or, more precisely, on the electromagnetic structure of the "region of the transition of A to B" can be extracted from a study of the probability for the decay $A\to B+l^++l^-$ as a function of the square of the effective mass of the lepton pair, $m^2_{l^+l^-}=q^2$. This probability, per unit interval of q^2, is called the "effective-mass spectrum" of the lepton pairs, $d\Gamma/dq^2$.

If the particles A and B could be considered to be structureless point objects, we could calculate the mass spectrum of the lepton pairs, $(d\Gamma/dq^2)$ very accurately by the methods of quantum electrodynamics. Actually, the complex structure of the particles alters this spectrum:

$$\frac{d\Gamma}{dq^2}=\frac{d\Gamma}{dq^2}\Big|_{point}|F_{AB}(q^2)|^2. \tag{1.6}$$

Comparing the measured spectrum of lepton pairs with the quantum-electrodynamics calculations for point particles, we can experimentally determine the transition form factor in the timelike region of momentum transfer.[1)]

In summary, by detecting the conversion decays of mesons, $A\to B+l^++l^-$, and by studying the effective-mass spectrum of the lepton pairs formed in these decays, we can measure the form factor which determines the electromagnetic structure of the region in which meson A converts into B. Of particular interest are the decays $A\to l^+l^-\gamma$ (which correspond to the internal conversion of a photon from the decay $A\to 2\gamma$, which is possible for neutral pseudoscalar mesons, for example). In this case the transition form factor describes the electromagnetic structure of the $A\to\gamma$ vertex, which a single hadron—the decaying meson A-enters. It is the electromagnetic properties of this hadron which are determined by the corresponding transition form factor.

We turn now to a detailed exposition of the results which have been obtained in studies of the conversion decays of the light neutral mesons π^0, η, η' and ω, for the most part at Serpukhov (Institute of High-Energy Physics)[7-9] and Geneva (CERN).[10]

2. STUDY OF THE ELECTROMAGNETIC STRUCTURE OF NEUTRAL LIGHT IN THE RARE CONVERSION DECAYS OF THESE PARTICLES

a) Spectra of lepton pairs in conversion decays of pseudoscalar and vector mesons[11-18]

The matrix elements of the conversion decays $A\to Bl^+l^-$ of vector and pseudoscalar mesons,

$$V\to Pl^+l^-, \tag{2.1}$$

$$P\to Vl^+l^-, \tag{2.2}$$

have the invariant form

$$M=4\pi\alpha i\underbrace{(f_{AB}(q^2)\,\epsilon^{\alpha\beta\gamma\delta}p_\alpha q_\beta e_\gamma)}_{A\to B\gamma_V\text{ transition}}\underbrace{\frac{1}{q^2}}_{\substack{\text{photon}\\\text{propagator}}}\underbrace{(\bar u\gamma_\delta u)}_{\substack{\text{Lepton}\\\text{current}}}. \tag{2.3}$$

Here and below, $f_{AB}(q^2)$ is the form factor of the transition $A\to B$; q_β is the 4-momentum of the virtual photon (of the

l^+l^- system); $q^2 = m^2_{l^+l^-}$; p_α is the 4-momentum of meson B; ε_γ is the polarization 4-vector of the vector particle V; $\varepsilon^{\alpha\beta\gamma\delta}$ is the antisymmetric unit tensor; m_A is the mass of the primary meson; m_B is that of the secondary meson; and $m_{l^+l^-}$ is the effective mass of the lepton pair; and m_l is the mass of the lepton.

We can thus derive the effective-mass spectrum of the lepton pairs in $A\to Bl^+l^-$ decays of the types in (2.1) and (2.2), normalized to the width of the corresponding radiative decay $A\to B\gamma$:

$$\frac{d\Gamma(A\to Bl^+l^-)}{dq^2\Gamma(A\to B\gamma)}=\frac{\alpha}{3\pi}\left(1-\frac{4m_l^2}{q^2}\right)^{1/2}\left(1+2\frac{m_l^2}{q^2}\right)\frac{1}{q^2}\times\left[\left(1+\frac{q^2}{m_A^2-m_B^2}\right)^2-\frac{4m_A^2q^2}{(m_A^2-m_B^2)^2}\right]^{3/2}\left|\frac{f_{AB}(q^2)}{f_{AB}(0)}\right|^2 \quad (2.4)$$

(for $V\to Pl^+l^-$ or $P\to Vl^+l^-$).

We introduce a normalized form factor for the transition A→B:

$$\frac{f_{AB}(q^2)}{f_{AB}(0)}=F_{AB}(q^2). \quad (2.5)$$

The normalization is

$$F_{AB}(0)=1. \quad (2.6)$$

Slightly different is the particular case of the conversion decay of a pseudoscalar meson (A = P), in which the secondary particle B is a γ ray:

$$P\to l^+l^-\gamma. \quad (2.7)$$

The corresponding radiative decay $P\to 2\gamma$ has two photons in its final state. The energy spectrum of the lepton pairs for decays of the type in (2.7) (normalized to the total probability for the radiative transition) is given by

$$\frac{d\Gamma(P\to l^+l^-\gamma)}{dq^2\Gamma(P\to 2\gamma)}=\frac{2\alpha}{3\pi}\sqrt{1-\frac{4m_l^2}{q^2}}\left(1+\frac{2m_l^2}{q^2}\right)\frac{1}{q^2}\left(1-\frac{q^2}{m_P^2}\right)^3|F_P(q^2)|^2; \quad (2.8)$$

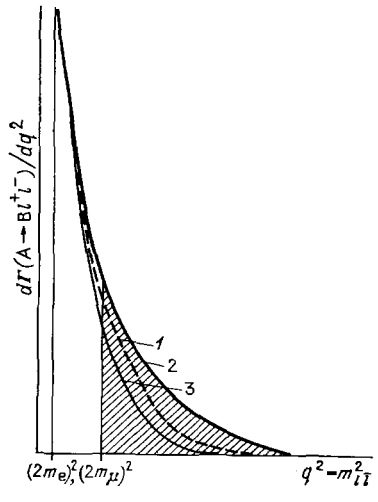

FIG. 3. Effect of the transition form factor on the mass spectrum of lepton pairs in conversion decays of mesons (schematic). Hatching—region of decay accompanied by the production of muon pairs; curve 1—mass spectrum for the decay of point particles ($F_{AB}=1$); 2—spectrum for $|F_{AB}(q^2)|^2>1$ (e.g., in the VDM); 3—spectrum for $F_{AB}(q^2)|^2<1$.

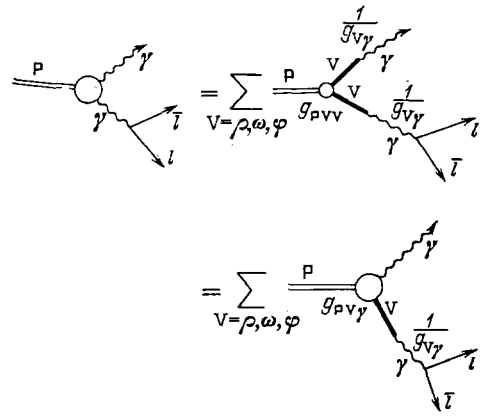

FIG. 4. Feynman diagrams for the form factor of a pseudoscalar meson in the VDM. For the description of the transition form factor, it is important to take into account vector dominance only for the virtual photon; the remainder reduces to a determination of the constant $g_{PV\gamma}$.

where m_P is the mass of pseudoscalar meson P, and $F_P(q^2)$ is the normalized transition form factor for decay (2.7).[2)] It is easy to see that the limit $m_B\to 0$ the right side of (2.4) becomes (1/2)×[the right side of 2.8)]. This difference of a factor of two is a consequence of the two possibliities for the choice of the virtual γ ray in the $P\to 2\gamma$ decay.

As we mentioned in the Introduction (§1), the electromagnetic transition form factor $f_{AB}(q^2)$ or $F_P(q^2)$ can be determined from experimental data on the mass spectrum of lepton pairs in the conversion decays of mesons after the quantum-electrodynamic factors have been taken out. The approach is shown schematically in Fig. 3. General considerations indicate that the effect of the form factor might be to either raise or lower the spectrum of lepton pairs from that calculated for point particles. To determine the order of magnitude and the sign of the expected effect, we can use the vector dominance model (VDM).

According to this model (Refs. 2, 19, and 20, for example), the electromagnetic current of the hadrons is proportional to the fields of the vector mesons $V=\rho,\omega,\varphi$:

$$J_\mu(x)=\sum_{V=\rho,\omega,\varphi}\frac{m_V^2}{2g_{V\gamma}}V_\mu(x). \quad (2.9)$$

The interaction of the photons with the hadrons occurs through virtual vector mesons. The coefficients $m_V^2/2g_{V\gamma}$ determine the constants of the transition of the vector mesons into photons.

In the vector dominance model the transition form factors in the conversion decays of mesons are described by the diagrams in Fig. 4. The form factor in this case is[21]

$$F_{AB}(q^2)=\frac{\sum_V(g_{ABV}/2g_{V\gamma})m_V^2(m_V^2-q^2-i\Gamma_Vm_V)^{-1}}{\sum_V(g_{ABV}/2g_{V\gamma})(1-i\Gamma_Vm_V)^{-1}}\approx\frac{\sum_V(g_{ABV}/2g_{V\gamma})[1-(q^2/m_V^2)]^{-1}}{\sum_V(g_{ABV}/2g_{V\gamma})} \quad (2.10)$$

(in the approximation of a small width Γ_V; here $V=\rho,\omega,\varphi$. Here g_{ABV} and $g_{V\gamma}$ are the corresponding interaction con-

TABLE I. Expected slopes of the form factors of certain neutral mesons in VDM.

Decay	Slope of form factor, $(dF_{AB}/dq^2)_{q^2\approx 0}$
$\pi^0 \to e^+e^-\gamma$	$\frac{1}{m_\rho^2}\left(\frac{1}{2}+\frac{1}{2}\frac{m_\rho^2}{m_\omega^2}\right)\approx\frac{0{,}99}{m_\rho^2}=1{,}7\ \text{GeV}^{-2}$
$\eta \to \mu^+\mu^-\gamma$	$\frac{1}{m_\rho^2}\frac{1+(1/9)(m_\rho^2/m_\omega^2)-\beta_\eta(\sqrt{2}/3)(m_\rho^2/m_\Phi^2)}{1+(1/9)-\beta_\eta(\sqrt{2}/3)}\approx\frac{1{,}1}{m_\rho^2}=1{,}8\ \text{GeV}^{-2}$
$\eta' \to \mu^+\mu^-\gamma$	$\frac{1}{m_\rho^2}\frac{1+(1/9)(m_\rho^2/m_\omega^2)+\beta_{\eta'}(\sqrt{2}/3)(m_\rho^2/m_\Phi^2)}{1+(1/9)+\beta_{\eta'}(\sqrt{2}/3)}=\frac{0{,}88}{m_\rho^2}=1{,}5\ \text{GeV}^{-2}$
$\omega \to \pi^0\mu^+\mu^-$	$\frac{1}{m_\rho^2}=1{,}7\ \text{GeV}^{-2}$

1. The values of the ratios of the constants g_{ABV} and $g_{V\gamma}$ in the quark model are:

$$\frac{1}{2g_{\rho\gamma}}:\frac{1}{2g_{\omega\gamma}}:\frac{1}{2g_{\varphi\gamma}}=1:\frac{1}{3}:\left(-\frac{\sqrt{2}}{3}\right),$$

$$\left.\begin{aligned} g_{\eta\rho\gamma}:g_{\eta\omega\gamma}:g_{\eta\varphi\gamma}&=1:\frac{1}{3}:(+\beta_\eta),\\ g_{\eta'\rho\gamma}:g_{\eta'\omega\gamma}:g_{\eta'\varphi\gamma}&=1:\frac{1}{3}:(-\beta_{\eta'}),\end{aligned}\right\}\quad g_{\pi^0\rho\gamma}:g_{\pi^0\omega\gamma}=1:3.$$

2. $\beta_\eta=\frac{2}{3}\left[(\sqrt{2}\cos\vartheta_P+\sin\vartheta_P)(\cos\vartheta_P-\sqrt{2}\sin\vartheta_P)^{-1}\right]\approx\begin{cases}0{,}50, & \vartheta_P=-18^\circ,\\ 0{,}65, & \vartheta_P=-10{,}5^\circ.\end{cases}$

3. $\beta_{\eta'}=\frac{4}{9}\beta_\eta^{-1}=\frac{2}{3}\left[(\cos\vartheta_P-\sqrt{2}\sin\vartheta_P)(\cos\vartheta_P\cdot\sqrt{2}+\sin\vartheta_P)^{-1}\right]\approx$

$\approx\begin{cases}0{,}89, & \vartheta_P=-18^\circ,\\ 0{,}68, & \vartheta_P=-10{,}5^\circ.\end{cases}$

Here ϑ_P is the mixing angle for pseudoscalar mesons (the difference between the possible values $\vartheta_P=-10.5^\circ$ and -18° has little effect on the slope of the form factor). For vector mesons, an ideal mixing is assumed, $\vartheta_V=\arcsin(1/\sqrt{3})=35.3^\circ$.

stants. At small momentum transfer we have

$$F_{AB}(q^2)\approx 1+q^2\left[\frac{dF_{AB}(q^2)}{dq^2}\right]\Big|_{q^2\approx 0}=1+q^2b_{AB}$$
$$=1+\frac{1}{6}q^2\langle r_{AB}^2\rangle. \quad (2.11)$$

The slope of the transition form factor is

$$b_{AB}=\frac{dF_{AB}}{dq^2}\Big|_{q^2\approx 0}=\frac{1}{m_\rho^2}\frac{\sum_V[(g_{ABV}/2q_{V\gamma})/(g_{AB\rho}/2g_{\rho\gamma})]\,m_\rho^2/m_V^2}{\sum_V[(g_{ABV}/2g_{V\gamma})/(g_{AB\rho}/2g_{\rho\gamma})]}; \quad (2.12)$$

here $\sqrt{\langle r_{AB}^2\rangle}=\sqrt{6(dF_{AB}/dq^2)|_{q^2\approx 0}}$ is a characteristic dimension associated with the region of the A→B transition. The interaction constants g_{ABV} and $G_{V\gamma}$ can be determined from the quark model and from experimental data on the decays A→BV, A→Bγ, V→l^+l^-.

Table I shows values of the ratios of these constants along with the corresponding predictions for the slopes of the transition form factors of neutral mesons.

These slopes are positive and approximately equal to $1/m_\rho^2$. The vector dominance model thus predicts the growth of the transition form factors with increasing mass of the lepton pair. The form factor can be approximated quite well in the form $F_{AB}(q^2)=[1-(q^2/\Lambda^2)]^{-1}$, where the characteristic mass is $\Lambda\approx m_\rho$ ($\Lambda^{-2}=(dF_{AB}/dq^2)_{q\approx 0}$). The predictions of the VDM will be discussed in more detail below. At this point, we regard these predictions as no more than purely phenomenological estimates, useful for analyzing experimental results on the transition form factors in conversion decays. Before we take up these results, we have a few comments.

a) The effect of the transition form factors increases with the mass of the meson and thus with the accessible region of momentum transfer. For example, estimates in the VDM show that the effect of the form factor on the effective-mass spectrum of electron pairs in the decay $\pi^0\to e^+e^-\gamma$ amounts to ~2% at the center of the spectrum and no more than 6% even at the highest accessible values of $m_{e^+e^-}^2$. For this reason, a study of the form factor of the π^0 meson is an especially difficult problem and requires a huge statistical base (10^4–10^5 events). By way of comparison we note that the expected effect of the form factor in the center of the effective-mass spectrum of $\mu^+\mu^-$ pairs in the decay $\eta\to\mu^+\mu^-\gamma$ is 26%, while at the largest values of $m_{\mu^+\mu^-}$ the form factor will increase the spectrum to a level nearly four times that of the quantum-electrodynamic calculations for point particles.

b) For decays accompanied by the production of electron pairs, radiative corrections proportional to $\alpha\ln^2(q^2/m_l^2)$ are important. The situation is further complicated by radiative processes in the material of the apparatus. Suffice it to say that at a total effective thickness of only 0.01 radiation length the number of background e^+e^- pairs which are

TABLE. II. Experimental results on conversion decays of neutral mesons.

Experiment and process studied	Experimental apparatus (in brief)	Experimental results
1. [23] (1961), $\pi^0 \to e^+e^-\gamma$	Liquid-hydrogen bubble chamber	$b_{\pi^0} = -8.5 \pm 5.5\ \text{GeV}^{-2}$. The errors are statistical. No radiative corrections have been made
2. [22] (1961), $\pi^0 \to e^+e^-\gamma$	Liquid-hydrogen bubble chamber. Statistical base: $N(\pi^0 \to e^+e^-\gamma) = 3071$	$b_{\pi^0} = -13.2 \pm 8.8\ \text{GeV}^{-2}$. Br $(\pi^0 \to e^+e^-\gamma) = (1.166 \pm 0.047) \cdot 10^{-2}$. The errors are statistical. No radiative corrections have been made.
3. [24] (1969), $\pi^0 \to e^+e^-\gamma$	Apparatus with optical spark chambers and NaI(Tl) shower spectrometers. The π^0 mesons are produced in the capture of π^- mesons in hydrogen. Statistical base: $N(\pi^0 \to e^+e^-\gamma) = 2200$	$b_{\pi^0} = 0.6 \pm 6.0\ \text{GeV}^{-2}$. The errors are statistical. No radiative corrections have been made.
4. [25] (1972), $\pi^0 \to e^+e^-\gamma$	Magnetic spectrometer	$b_{\pi^0} = 0{,}9 \pm 5{,}5\ \text{GeV}^{-2}$
5. [10] (1978), $\pi^0 \to e^+e^-\gamma$	Magnetic spectrometer with wire spark chambers. The electrons are identified by gas-filled Cherenkov counters (Fig. 5). The source of the "tagged" π^0 mesons is the in-flight decay $K^+ \to \pi^+ + \pi^0$, $\pi^0 \to e^+e^-(\gamma)$. The γ rays were not detected and were instead reconstructed from the kinematics. Statistical base: $N(\pi^0 \to e^+e^-\gamma) = 20\,981$ in the region $0.3 < (m_{e^+e^-}/m_{\pi^0}) < 0.9$	$b_{\pi^0} = 5.5 \pm 1.6\ \text{GeV}^{-2}$. The errors are statistical. Radiative corrections have been made; they increase the slope b_{π^0} by a factor ~ 2.
6. [26] (1981), $\pi^0 \to e^+e^-\gamma$	Double-arm spectrometer: shower spectrometer for detecting γ rays (one arm); magnetic spectrometer with proportional chambers for detecting e^+e^- pairs (the other arm). Extrapolation to a zero target thickness to eliminate external γ conversion.	Br $(\pi^0 \to e^+e^-\gamma) = [1.25 \pm 0.04\ (\text{statist.})] \pm 0.01(\text{syst.})] \cdot 10^{-2}$ Radiative correctons have been made.
7. [27] (1973), $\eta \to e^+e^-\gamma$	Bubble chamber	$b_\eta = -2{,}6 \pm 5{,}7\ \text{GeV}^{-2}$
8. [28] (1975), $\eta \to e^+e^-\gamma$	Magnetic spectrometer with optical spark chambers. The electrons are identified by gas-filled Cherenkov counters. Statistical base: $N(\eta \to e^+e^-\gamma) = 50$ in the region $0.1 < (m_{e^+e^-}/m_\eta) < 0.7$	$b_\eta = -0.7 \pm 1.5\ \text{GeV}^{-2}$. The errors are statistical; no radiative corrections have been made; the authors assert that these corrections are small
9. [7-9] (1980), $\eta \to \mu^+\mu^-\gamma$, $\eta' \to \mu^+\mu^-\gamma$, $\omega \to \pi^0\mu^+\mu^-$	The Lepton-G apparatus (Fig. 6). Magnetic spectrometer with proportional and wire spark chambers to detect muons and a hodoscopic γ spectrometer to detect γ rays. The energies of all the secondary particles are measured; muons and γ rays are identified. Complete reconstruction of the kinematics of the decay. Statistical base: $N(\eta \to \mu^+\mu^-\gamma) = 600$, $N(\eta' \to \mu^+\mu^-\gamma) = 33$, $N(\omega \to \pi^0\mu^+\mu^-) = 60$	$\eta \to \mu^+\mu^-\gamma$ { $b_\eta = 1{,}9 \pm 0{,}4\ \text{GeV}^{-2}$; Br $= (3{,}1 \pm 0{,}4) \cdot 10^{-4}$ } $\eta' \to \mu^+\mu^-\eta$ { $b_{\eta'} = 1{,}7 \pm 0{,}4\ \text{GeV}^{-2}$; Br $= (8{,}9 \pm 2{,}4) \cdot 10^{-5}$ } $\omega \to \pi^0\mu^+\mu^-$ { $b_{\omega\pi^0} = 2{,}4 \pm 0{,}2\ \text{GeV}^{-2}$; Br $= (9{,}6 \pm 2{,}3) \cdot 10^{-5}$ } The errors include both statistical and systematic errors. The radiative corrections for the muon decays are negligibly small.

In Refs. 7–9 (entry 9), in the determination of $b = (dF/dq^2)|_{q^2=0}$ the transition form factor was parametrized over the entire range of q^2 studied in the pole approximation, $F(q^2) = [1 - (q^2/\Lambda^2)]^{-1}$ (for the η' meson in the region $q^2 \lesssim 0.4\ \text{GeV}^2$). Here $b = \Lambda^{-2}$. In all other studies the form factor has been parametrized in the linear approximation $F(q^2) = 1 + bq^2$, which holds only for the decay $\pi^0 \to e^+e^-\gamma$ (because of the small limiting values of q^2 in this process).

formed in this material from the external conversion of γ rays from the radiative decays $P \to 2\gamma$ will be the same as the number formed in the decays $P \to e^+e^-\gamma$. For decays accompanied by the production of muon pairs the radiative corrections and the external radiation effects usually are negligibly small.

c) Comparing the conversion decays of given meson with the production of electron and muon pairs, we estimate that the process involving the production of electron pairs has a probability an order of magnitude higher than that for the corresponding muon decay. However, this difference has almost no effect on the accuracy of the measurements of the transition form factors: the difference in probabilities results from the part of the electron-pair spectrum with small effective masses [$< (2m_\mu)$; see Fig. 3], which contributes essentially nothing to the parameters of the form factor.

d) For conversion decays accompanied by the emission of muon pairs, the form factor should have an important effect even on the partial widths of these decays, increasing them by a factor of 1.5 or 2 (according to the VDM predictions).

We conclude from all this that processes accompanied by the production of muon pairs have important methodological advantages for a study of transition form factors in the conversion decays of mesons.

b) Experimental data on the transition form factors of neutral light mesons

1) Results of research on the conversion decays of mesons

Experimental information has now been acquired on the following leptonic conversion decays of neutral mesons:

$$\pi^0 \to e^+e^-\gamma, \tag{2.13}$$

$$\eta \to e^+e^-\gamma, \tag{2.14}$$

$$\eta \to \mu^+\mu^-\gamma, \tag{2.15}$$

$$\eta' \to \mu^+\mu^-\gamma, \tag{2.16}$$

$$\omega \to \pi^0\mu^+\mu^-. \tag{2.17}$$

The results of all the experimental work in this field are summarized in Table II. The old measurements of the decays (2.13) (Refs. 22–25) and (2.14) (Refs. 27 and 28) have a very limited statistical base; no radiative corrections were made; they have a significant background from γ conversion in the target and in the material of the apparatus; and they have other shortcomings. These studies are thus purely qualitative. Reasonably accurate measurements, providing a basis for a quantitative study of the transition form factors of mesons, have been carried out only in recent experiments at CERN [a study[10] of the decay (2.13)] and at Serpukhov [the decays[7–9] (2.15)–(2.17)].

For π^0 mesons, because of their small mass, the decay accompanied by the emission of an electron pair, $\pi^0 \to e^+e^-\gamma$, is the only decay process in which the transition form factor can be studied. As mentioned earlier, external radiative processes and also radiative corrections are important in experiments carried out to analyze electron pairs. In order to reduce the importance of radiative processes, an effort should be made to minimize the material of the apparatus (primarily the target in which the π^0 mesons are produced). In some CERN experiments[10] the source of π^0 mesons was the in-flight decay of K^+ mesons of the primary beam by the channel $K^+ \to \pi^+\pi^0$. As a result of measurements of the kinematic parameters of the K^+ and π^+ mesons, it was possible to single out "tagged" π^0 mesons with known initial momenta. The experimental apparatus is shown schematically in Fig. 5.

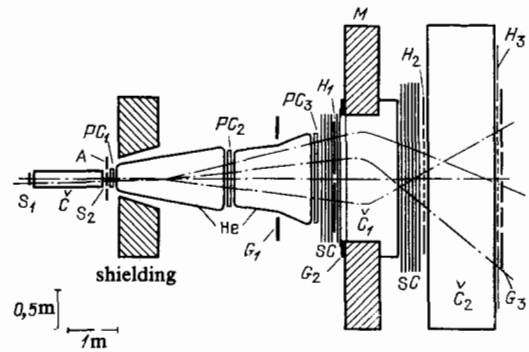

FIG. 5. The experimental apparatus used in the study of the decay $\pi^0 \to e^+e^-\gamma$. S_1,S_2, A—scintillation counters; H_1–H_3—scintillation hodoscopes; G_1–G_3—counter sandwiches consisting of a scintillator and lead; C,C_1,C_2—gas-filled Cherenkov counters; SC—wire spark chambers; PC—proportional chambers; M—magnet. The decay region is filled with helium.

As a result of this experiment, 20 981 $\pi^0 \to e^+e^-\gamma$ decay events were selected with the mass of the e^+e^- pair in the interval $0.3 < (m_{e^+e^-}/m_{\pi^0}) < 0.9$. In this interval of effective masses, the background from other processes does not exceed 0.3% and does not distort the shape of the distribution in q^2. Study of the shape of the electron-pair spectrum with the help of (2.8) made it possible to determine the transition form factor of the π^0 meson, which was approximated by the linear expression

$$F_{\pi^0}(q^2) = F_{\pi^0}(q^2;\ 0;\ m^2_{\pi^0}) = 1 + b_{\pi^0} q^2. \tag{2.18}$$

The linear approximation is quite good here because of the small value of the maximum square momentum transfer: $q^2 < 0.02\ \text{GeV}^2$. The following value was found for the slope of the form factor at $q^2 \approx 0$:

$$b_{\pi^0} = \frac{dF_{\pi^0}}{dq^2}\bigg|_{q^2 \approx 0} = 5.5 \pm 1.6\ \text{GeV}^{-2} \tag{2.19}$$

(the indicated error is the statistical error). The radiative corrections played a very important role, altering the slope of the form factor by a factor of two (without these corrections we would have $b_{\pi^0} = 2.7 \pm 1.6\ \text{GeV}^{-2}$). The slope of the form factor is about 2.5 standard deviations above the corresponding VDM predictions.

The most accurate determination of the relative probability for decay (2.13) was carried out in an experiment[26] at the LAMPF meson factory at Los Alamos:

$$\text{Br}(\pi^0 \to e^+e^-\gamma)$$

$$= [1.25 \pm 0.04\ (\text{statist.}) \pm 0.01\ (\text{syst.})] \cdot 10^{-2}. \tag{2.20}$$

In a series of experiments carried out on the Lepton-G apparatus[7–9] at Serpukhov, decays (2.15)–(2.17) were detected for

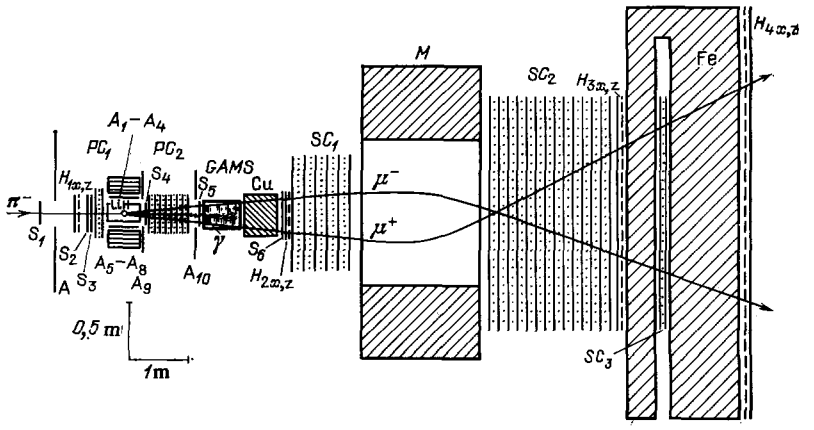

FIG. 6. The Lepton-G experimental apparatus. Beam particle detectors: S_1–S_3—Scintillation counters; $H_{1x,z}$—scintillation hodoscope; PC_1—proportional chamber. System for identifying exclusive processes: A—antihalo scintillation counters; LiH—50-cm target; A_1–A_4,A_9,A_{10}—guard scintillation counters; A_5–A_8—shower counter sandwiches S_4,S_5—scintillation counters for identifying interactions in the target; PC_2—proportional chambers for measuring the coordinates of the secondary charged particles; *GAMS*—γ hodoscopic spectrometer with 64 lead glass cells; Cu—copper filter (700 mm); S_6—counter for a preliminary sampling of penetrating particles. Wide-aperture secondary-particle magnetic spectrometer: M—magnet; $H_{2x,z}$,$H_{3x,z}$—hodoscopes; SC_1 (10 chambers) and SC_2 (20 chambers)—wire spark chambers. Muon detector: $H_{2x,z}$—hodoscopes; SC_3—wire spark chambers alternating with iron plates with a total thickness of 2m.

the first time, and data were obtained on the electromagnetic structure of the η, η', and ω mesons. This apparatus is a composite spectrometer with makes it possible to detect effectively processes accompanied by the simultaneous emission of muon pairs and γ rays and to carry out a complete kinematic reconstruction of all the secondary particles. The Lepton apparatus is shown schematically in Fig. 6. The sources of the mesons in this study were the quasi-two-particle exclusive reactions

$$\pi^- + p \to M + n \ (M = \eta, \eta', \omega) \qquad (2.21)$$

in the region 25–33 GeV of the primary momentum of the π^- mesons.[3)] These reactions provide favorable background conditions for seeking and studying rare electromagnetic decays.

Over the course of the measurements, about $5\cdot10^{11}$ π^- mesons passed through the apparatus. This figure corresponds to the production of $2\cdot10^7$ η mesons and 10^7 η' and ω mesons in binary reactions (2.21). For the analysis, events were selected with a kinematics corresponding to the exclusive reactions

$$\pi^-p \to \mu^+\mu^-\gamma n, \qquad (2.22)$$
$$\to \mu^+\mu^-\gamma\gamma n, \qquad (2.23)$$
$$\to \mu^+\mu^- n. \qquad (2.24)$$

Decays (2.15)–(2.17) were detected in an analysis of the effective-mass spectra of the $\mu^+\mu^-\gamma$ and $\mu^+\mu^-\pi^0$ states; they were seen as clearly defined peaks in the mass region of the mesons of interest (Figs. 7 and 8). The events lying in these peaks were then used for a study of the mass spectrum $d\Gamma/dq^2$ of the muon pairs.

Figure 9 shows experimental values of the square form factor of the η meson, $|F_\eta(q^2)|^2$. These values were determined for the selected events of decay (2.15) as the ratio of the measured spectrum $d\Gamma/dq^2$ to the spectrum calculated by the Monte Carlo method from (2.8) with $F = 1$ and with allowance for the efficiency of the apparatus. In this particular case, Eq. (2.8) becomes

$$\frac{d\Gamma(\eta \to \mu^+\mu^-\gamma)}{dq^2\Gamma(\eta \to 2\gamma)} = \frac{2}{3}\frac{\alpha}{\pi}\frac{1}{q^2}\left(1-\frac{q^2}{m_\eta^2}\right)^3 \times \left(1+\frac{2m_\mu^2}{q^2}\right)\sqrt{1-\frac{4m_\mu^2}{q^2}}\,|F_\eta(q^2)|^2; \qquad (2.25)$$

here $q^2 - m^2$ is the square of the mass of the muon pair, m_μ and m_η are the masses of the muon and of the η meson, and $F_\eta(q^2)$ is the transition form factor of the η meson, parametrized in the pole approximation

$$F_\eta(q^2) = F_\eta(q^2;\ 0;\ m_\eta^2) = \left(1-\frac{q^2}{\Lambda_\eta^2}\right)^{-1}. \qquad (2.26)$$

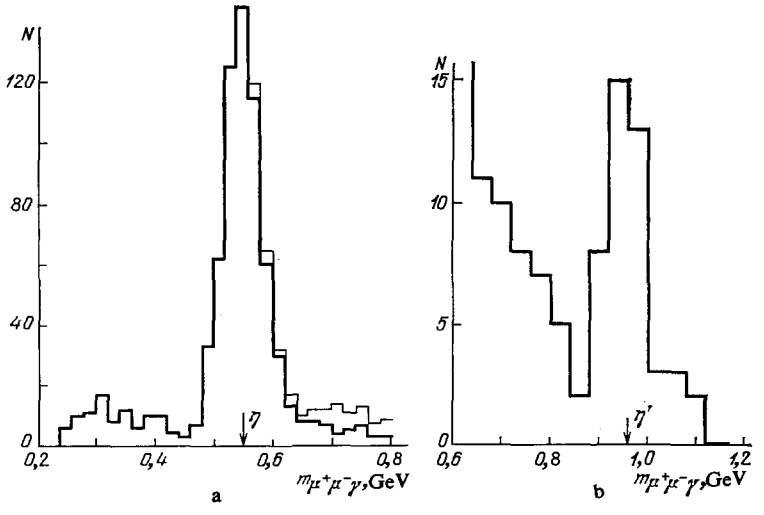

FIG. 7. a: Mass spectrum of the $\mu^+\mu^-\gamma$ system in reaction (2.22). Peak—the decay $\eta \to \mu^+\mu^-\gamma$; arrow—tabulated mass of the η meson; light histogram—all events; heavy histogram—events with $m^2_{\mu^+\mu^-} < 0.24$ GeV^2, used to determine the transition form factor for the η meson; N—number of events per 20-MeV mass interval. b: Mass spectrum of the $\mu^+\mu^-\gamma$ system in reaction (2.22) in the region above m_η. Arrow—Tabulated mass of the η' meson; N—number of events per 40-MeV mass interval.

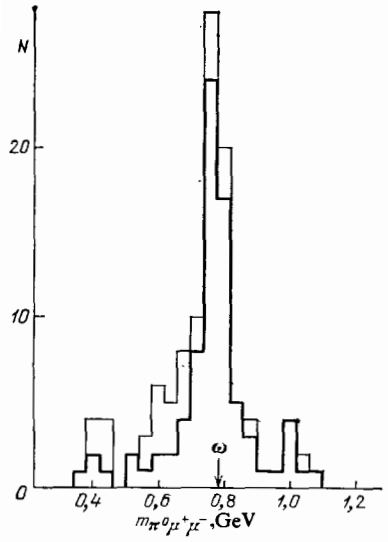

FIG. 8. Mass spectrum of the $\mu^+\mu^-\pi^0$ system in reaction (2.23) for events with $m^2_{\mu^+\mu^-} \leqslant 0.4$ GeV^2 (these events were subsequently used to measure the transition form factor). Peak—the decay $\omega \to \pi^0\mu^+\mu^-$; arrow—tabulated mass of the ω meson; N—number of events per 40-MeV mass interval; outer and inner lines of the histograms—thresholds of $(E_\gamma)_{\text{thr}} = 1$ and 1.4 GeV, respectively, in the energy of the γ rays [the background conditions of the experiment improve with increasing $(E_\gamma)_{\text{thr}}$].

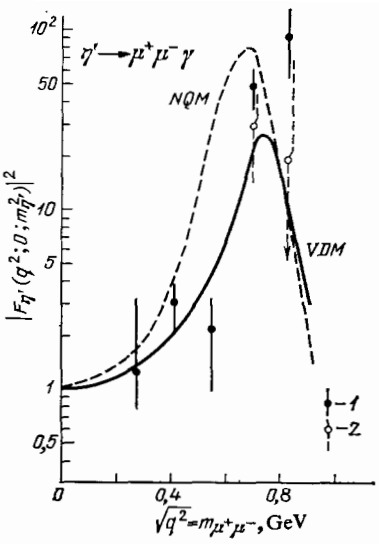

FIG. 10. Measurements of the electromagnetic transition form factor of the η' meson in decay (2.16). 1—Experimental values of the square of the form factor, $|F_{\eta'}(q^2;0;m^2_{\eta'})|^2$; 2—the same, but with the maximum correction for a 20% background in the $\eta' - \mu^+\mu^-\gamma$ peak (Fig. 7b; it is assumed that the entire background lies in the mass region of the ρ meson); solid curve—VDM predictions; dashed curve—predictions based on a nonlocal quark model (NQM).

The characteristic mass Λ_η is found to be

$$\Lambda_\eta = 0.72 \pm 0.09 \text{ GeV}. \tag{2.27}$$

The slope of the form factor at $q^2 \approx 0$ is

$$b_\eta = \frac{dF_\eta}{dq^2}\Big|_{q^2\approx 0} = \frac{1}{\Lambda^2_\eta} = 1.9 \pm 0.4 \text{ GeV}^{-2}. \tag{2.27'}$$

It can be seen from (2.27) and (2.27') that the experimental data on $F_\eta(q^2)$ agree well with the VDM (see also Fig. 16 below). An agreement of this sort with the VDM for transition form factors was first attained in Ref. 7 (see Fig. 14 below).

Figure 10 shows data on the experimental square of the transition form factor of the η' meson, $|F_{\eta'}(q^2;0;m^2_{\eta'})|^2$. The procedure for measuring the form factor here is completely identical to that which was used in analyzing the electromagnetic structure of the η meson.

The slope of the η' form factor at $q^2 \approx 0$ is

$$b_{\eta'} = \frac{dF_{\eta'}}{dq^2}\Big|_{q^2\approx 0} = 1.7 \pm 0.4 \text{ GeV}^{-2}. \tag{2.28}$$

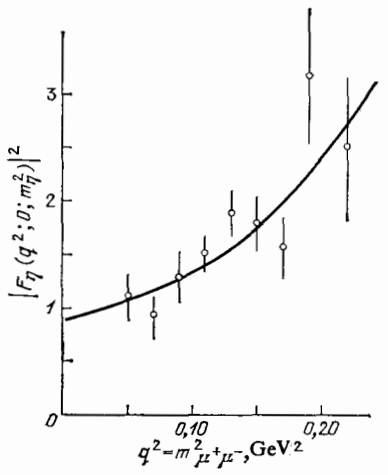

FIG. 9. Measurements of the electromagnetic transition form factor of the η meson in decay (2.15). Points—experimental values for $|F_\eta(q^2;0;m^2_\eta)|^2$; curve—fit of the experimental data by the pole function $K[1 - (q^2/\Lambda^2_\eta)]^{-2}$, where $\Lambda_\eta = 0.72 \pm 0.09$ GeV, and the coefficient K incorporates the error in the absolute normalization of the results of the measurement of $|F_\eta|^2$.

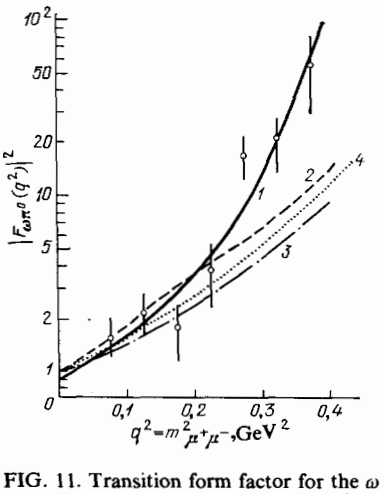

FIG. 11. Transition form factor for the $\omega - \pi^0$ vertex in decay (2.17). Points—experimental values of $|F_{\omega\pi^0}(q^2)|^2$; 1—fit of the experimental data by a pole function $K[1 - (q^2/\Lambda^2_\omega)]^{-2}$ (the coefficient K incorporates the uncertainty in the absolute normalization of the experimental quantities; $\Lambda_\omega = 0.65 \pm 0.03$ GeV); 2—prediction of the model of Ref. 49 with a modified ρ propagator; 3—VDM prediction; 4—prediction of the nonlocal quark model.[46]

The behavior of the transition form factor of the η' meson reflects an interesting physical phenomenon: For the decay $\eta' \to \mu^+\mu^-\gamma$, the ρ and ω poles lie in the physical region for the spectrum of muon pairs. The data on the transition form factor of the η' meson and the VDM predictions (Fig. 10) are in qualitative agreement. A more detailed analysis is not possible at present because of the limited statistical base of events (2.16).

Experimental data on the square of the transition form factor of the $\omega - \pi^0$ vertex in decay (2.17), $|F_{\omega\pi^0}(q^2)|^2$, are shown in Fig. 11. These results were found by the same method as we used for the form factor of the η meson. To describe the spectrum of muon pairs in this case, we used expression (2.4), parametrizing the form factor in the pole approximation [see (2.26)]. The characteristic mass Λ_ω is found to be

$$\Lambda_\omega = 0.65 \pm 0.03 \text{ GeV}. \tag{2.29}$$

The slope of the form factor is

$$b_{\omega\pi^0} = \frac{dF_{\omega\pi^0}}{dq^2}\bigg|_{q^2\approx 0} = \Lambda_\omega^{-2} = 2.4 \pm 0.2 \text{ GeV}^{-2}. \tag{2.29'}$$

In the VDM the transition form factor $F_{\omega\pi^0}(q^2)$ is governed by the ρ pole alone. We thus have $\Lambda_{\text{VDM}} = m_\rho$, which differs from the measured value by four standard deviations. At large masses $m_{\mu^+\mu^-}$ the form factor increases much more rapidly than is predicted by the VDM (Fig. 11).

The branching ratios for decays (2.15)–(2.17) have been determined; the results are shown in Table II and also in Table III below, which also summarizes the data on the slopes of the transition form factors. The following procedure was used to reduce the systematic errors stemming from the absolute normalization of the scale in determining the partial probabilities for events (2.15)–(2.17), measured in a common experiment. The relative probability for the decay $\eta \to \mu^+\mu^-\gamma$ was found by integrating the spectrum of muon pairs $d\Gamma(\eta \to \mu^+\mu^-\gamma)/dq^2\Gamma(\eta \to 2\gamma)$, determined from (2.25) with the help of experimental data on the transition form factor of the η meson [i.e., relations (2.26)–(2.27)]. The results are

$$\frac{\Gamma(\eta \to \mu^+\mu^-\gamma)}{\Gamma(\eta \to 2\gamma)} = (7.9 \pm 1.0)\cdot 10^{-4}, \tag{2.30}$$

$$\text{Br}(\eta \to \mu^+\mu^-\gamma) = \frac{\Gamma(\eta \to \mu^+\mu^-\gamma)}{\Gamma(\eta \to \text{anything})} = (3.1 \pm 0.4)\cdot 10^{-4} \tag{2.30'}$$

(the indicated error includes the systematic error also.) This is a more accurate value than that which was found from direct measurements ($\text{Br}(\eta \to \mu^+\mu^-\gamma) = (2.9 \pm 0.75)\cdot 10^{-4}$), where the error is due to the uncertainty in the absolute normalization. If the η meson were a point particle, then the quantity $\Gamma(\eta \to \mu^+\mu^-\gamma)/\Gamma(\eta \to 2\gamma)$ would be determined with tremendous precision from quantum electrodynamics [from expression (2.25)]. The entire error in (2.30) is due to errors in the measurements of the form factor $F_\eta(q^2)$. We should emphasize that the parameter Λ_η for the form factor of the η meson could be determined without any absolute normalization [i.e., without using the point $|F_\eta(0)|^2 = 1$ in the fit (Fig. 9)]. The value found by this approach, (Λ_η) (without normalization), agrees with Λ_η in (2.27). Consequently, the relative probability (2.30') does not depend in any way on a preliminary absolute normalizatin of the number of detected events.[4)] On the contrary, it was itself subsequently used for a more accurate normalization of other experimental results, including results on the partial probabilities $\text{Br}(\eta' \to \mu^+\mu^-\gamma)$ and $\text{Br}(\omega \to \pi^0\mu^+\mu^-)$ (see also Sec. 3).

The experimental values of the branching ratios for the conversion decays (2.15)–(2.17) are significantly larger than the calculated values found without consideration of the electromagnetic structure of the mesons (i.e., for form factors $F = 1$), and they agree reasonably well with the VDM predictions.

2) Transition form factors and experiments in e^+e^- beams

We turn now to the possibility of studying the transition form factors of neutral mesons in various processes in colliding e^+e^- beams. In these experiments, we can obtain data on the form factors in a kinematic region different from that involved in the conversion decays. All such measurements thus complement each other.

In recent experiments with "tagged photons" carried out at the PETRA e^+e^- storage ring with the PLUTO superconducting magnetic solenoidal spectrometer, the η' production reaction

$$e^+e^- \to e^+e^-\gamma_V\gamma_V = e^+e^-\eta' \tag{2.31}$$

was studied, with all the η' mesons and electrons in the final state being detected.[29] The cross section for this process is determined by the $\gamma_V\gamma_V$ collisions of virtual photons with known values of q_1^2 and q_2^2 (Fig. 12a). These 4-momenta lie in the spacelike region, and their values are determined by measuring the energy and emission angle of the corresponding

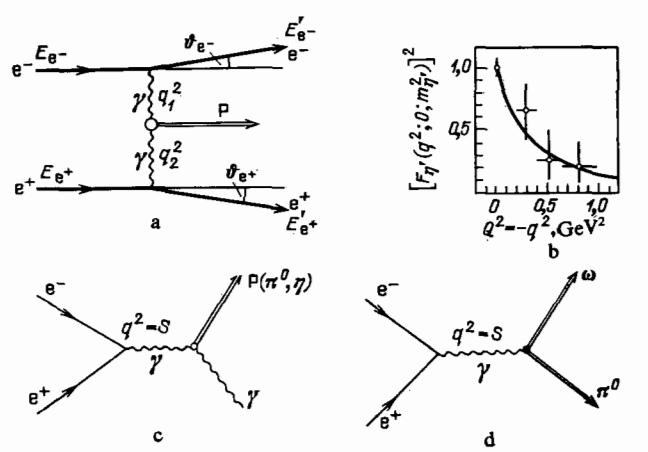

FIG. 12. Study of transition form factors of neutral mesons in experiments in colliding e^+e^- beams. a: Feynman diagram for the production of pseudoscalar mesons P in $\gamma_V\gamma_V$ collisions (γ_V is a virtual photon) in the reaction $e^+e^- \to e^+e^-\gamma_V\gamma_V + e^+e^-P$ [q_1^2 and q_2^2 are the squares of the 4-momenta of the virtual photons; $q^2 = -4EE'\sin^2(\vartheta/2) < 0$ are spacelike momenta; E and E' are the initial and final energies of the electron; ϑ is the emission angle of the secondary electron]. b: Results of a study of the transition form factor of the η' meson, $|F_{\eta'}(q^2;0;m_{\eta'}^2)|^2$, in the spacelike region in the reaction $e^+e^- \to e^+e^-\eta'$ in an experiment with a single tagging of virtual photons[29] [the solid curve is the VDM prediction; see (2.33) (an approximate expression); $Q^2 = -q^2 > 0$]. c: Feynman diagram for the reaction $e^+e^- \to \gamma P(P = \eta, \pi^0)$. d: Feynman diagram for the reaction $e^+e^- \to \omega\pi^0$.

secondary electron (this procedure is called the "tagging" of a virtual photon). As follows from Refs. 6 and 29, the cross section for the production of pseudoscalar mesons in $\gamma\gamma$ collisions is

$$\sigma(q_1^2;\ q_2^2;\ s)_{\gamma\gamma}=\frac{4\pi^2(\nu^2-m_P^2\tilde{Q}^2)\alpha^2\,|f_P(q_1^2;\ q_2^2;\ m_P^2)|^2\sqrt{s}\,\Gamma}{\sqrt{X}\,[(s-m_P^2)^2+\Gamma^2m_P^2]}. \tag{2.32}$$

Here $X=(q_1q_2)^2-q_1^2\cdot q_2^2$; $\tilde{Q}=(1/2)\ (q_1-q_2)$; $\nu=\tilde{Q}K$; $K=q_1+q_2$ is the 4-momentum of the pseudoscalar meson P; m_P and Γ are its mass and width; $\sqrt{s}$ is the invariant mass of the $\gamma\gamma$ system; and $\alpha=e^2/4\pi=1/137$. The transition form factor $f_P(q_1^2;q_2^2;m_P^2)$ is related to the radiative width of the P$\to 2\gamma$ decay, $\Gamma_{\gamma\gamma}$, by $\Gamma_{\gamma\gamma}=(1/4)\pi\alpha^2|f_P(0;\ 0;\ m_P^2)|^2m_P^2$. As before, we examine the normalized form factors [see (2.5)] $F_P(q_1^2;q_2^2;m_P^2)=f_P(q_1^2;q_2^2;m_P^2)/f_P(0;0;m_P^2)$. The cross section $\sigma_{\gamma\gamma}(q_1^2;q_2^2;s)$ is related to the cross section for an e^+e^- reaction of the type in (2.31) by means of the familiar expression for the "virtual-photon luminosity function" $L(q_1^2;\ q_2^2;\ s)$:

$$\sigma(e^+e^-\to e^+e^-\eta')=\int\sigma(q_1^2;\ q_2^2;\ s)_{\gamma\gamma}L(q_1^2;\ q_2^2;\ s)\,ds\,dq_1^2\,dq_2^2.$$

If the experiments are carried out without a detection of the electrons in the final state, (2.31) (i.e., if there is no tagging of the γ rays), the virtual photons will be near the mass shell ($q_1^2\approx q_2^2\approx 0$) and will be nearly real. In this case, (2.32) becomes

$$\sigma_{\gamma\gamma}(q_1^2\approx 0;\ q_2^2\approx 0)=\sigma_{\gamma\gamma}$$

$$=\frac{8\pi}{m_P}\sqrt{s}\,\Gamma_{\gamma\gamma}\Gamma\,[(s-m_P^2)^2+\Gamma^2m_P^2]^{-1}. \tag{2.32'}$$

Under these kinematic conditions, reaction (2.31) is used to measure the radiative width of the meson, $\Gamma(P\to\gamma\gamma)=\Gamma_{\gamma\gamma}$. When one or two electrons are detected in the final state (single or double tagging of the virtual photons), on the other hand, the kinematics of the experiment can be chosen in such a way that the squares of the 4-momenta carried by the photons change, so that the meson transition form factor $F_P(q_1^2;\ q_2^2;\ m_P^2)$ can be studied. Since the detection of the secondary electrons reduces the luminosity substantially, reaction (2.31) was studied with the PLUTO apparatus only with single tagging of the virtual photons.

For the detection of the η' meson, the decay channel $\eta'\to\rho^0\gamma\to\pi^+\pi^-\gamma$ of this meson was used, with the branching ratio $\mathrm{Br}(\eta'\to\rho^0\gamma)=0.300\pm 0.016$. The measurements were carried out under conditions such that both virtual photons were near the mass shell ($q_1^2\approx q_2^2\approx 0$; the recoil electrons were not detected) and also under conditions such that the secondary electrons were detected. In the latter case, the square of the momentum transfer carried by the virtual photon varied in the spacelike region $0>q^2>-1\ \mathrm{GeV}^2$. A total of 245 ± 16.5 events of reaction (2.31) were detected in experiments without tagging, and 35 ± 9 events were detected in experiments in which one of the photons was tagged. The two-photon radiative width was determined: $\Gamma(\eta'\to 2\gamma)=[3.80\pm 0.26\ (\text{statist.})\ \pm 0.43\ (\text{syst.})]$ keV. The transition form factor $F_{\eta'}(q^2;\ 0;\ m_{\eta'}^2)$ was also measured; from the results (Fig. 12b), we see that the behavior of the transition form factor of the η' meson in the spacelike region agrees with the VDM predictions:

$$F_{\eta'}(q^2;\ 0;\ m_{\eta'}^2)\approx\left(1-\frac{q^2}{m_\rho^2}\right)^{-1}=\left(1+\frac{Q^2}{m_\rho^2}\right)^{-1} \tag{2.33}$$

(here[5] $Q^2=-q^2>0$). the results of the colliding-beam experiments join well with data on the transition form factor of the η' meson in the timelike region (obtained from an analysis of the conversion decay $\eta'\to\mu^+\mu^-\gamma$).

The transition form factors of the neutral mesons can also be studied in the reactions $e^+e^-\to\pi^0\gamma;\ \eta\gamma;\ \omega\pi^0$; etc. (see the diagrams in Figs. 12c and 12d). The amplitudes for these processes are proportional to the form factors of the Pγ or $\omega\pi^0$ vertices—in the region of large timelike momentum transfer (see, for example, Fig. 13 below). A study of such reactions extends the region in which transition form factors have been studied beyond that corresponding to data on conversion decays.

The cross sections for $e^+e^-\to\pi^0\gamma$ or $e^+e^-\to\eta\gamma$ processes must be very small (10^{-34}–10^{-35} cm^2), so that corresponding experiments are exceedingly difficult. For the reaction $e^+e^-\to\omega\pi^0$, however, the cross sections are expected to be of the order of 10 nb, and the situation is more favorable. The first experiments have indeed already been carried out. The most reliable results were obtained in measurements in the neutral detector of the Institute of Nuclear Physics, Novosibirsk, at the VÉPP-2M e^+e^- storage ring.[30] This neutral detector included a calorimeter consisting of 168 scintillation counters using NaI(Tl) crystals and shower proportional counters (positioned inside the calorimeter) to

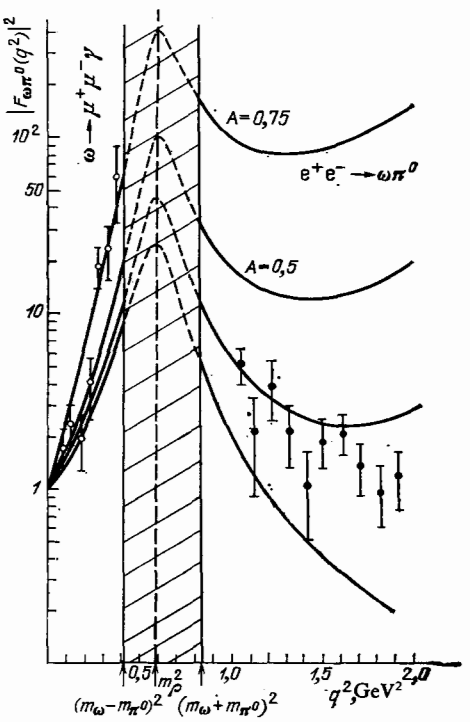

FIG. 13. Results of a study of the transition form factor of the $\omega\pi^0$ vertex in the decay[9] $\omega\to\pi^0\mu^+\mu^-$ and in the reaction[30] $e^+e^-\to\omega\pi^0$. The curves show the predictions of the model of generalized vector dominance with allowance for the $\rho(770)$ and $\rho'(1600)$ mesons [see (2.36)]: $A=-(g_{\rho'\omega\pi}/2g_{\rho'\gamma})(g_{\rho\omega\pi}/2g_{\rho\gamma})^{-1}$. The momentum-transfer region $(m_\omega-m_{\pi^0})^2<q^2<(m_\omega+m_{\pi^0})^2$ is forbidden by the kinematics of the processes under study (the "nonphysical region").

measure the photon emission angles. The total solid angle subtended by the detector was $0.65 \cdot 4\pi$ sr.

The reaction $e^+e^- \to \omega\pi^0$ was identified on the basis of the decay $\omega \to \pi^0\gamma \to 3\gamma$, which was detected in the detector along with γ rays from the decay of the π^0 meson. The cross section $\sigma(e^+e^- \to \omega\pi^0)$ was measured over the energy interval $1 \leqslant \sqrt{s} \leqslant 1.4$ GeV. The magnitude of the cross section is related to the form factor of the $\omega\pi^0$ vertex by[31]

$$\sigma_{e^+e^- \to \omega\pi^0}(s) = \frac{4\pi}{3}\frac{\alpha^2}{s^2}\rho_\omega |f_{\omega\pi^0}(s)|^2,$$

where

$$\rho_\omega = 4\sqrt{s}\left\{[s-(m_\omega+m_{\pi^0})^2][s-(m_\omega-m_{\pi^0})^2]\frac{1}{4s}\right\}^{3/2}.$$

The $\omega\pi^0$ transition form factor for $s = 0$ is determined by the radiative width of the $\omega \to \pi^0\gamma$ decay, $\Gamma(\omega \to \pi^0\gamma) = (4/3)\alpha p_0^3 |f_{\omega\pi^0}(0)|^2$, where $p_0 = (m_\omega^2 - m_{\pi^0}^2)/2m_\omega$ is the energy of the γ ray. Consequently, the normalized transition form factor $F_{\omega\pi^0}(s) = f_{\omega\pi^0}(s)/f_{\omega\pi^0}(0)$ is determined from the expression

$$|F_{\omega\pi^0}(s)|^2 = \left|\frac{f_{\omega\pi^0}(s)}{f_{\omega\pi^0}(0)}\right|^2 = \frac{\sigma_{e^+e^- \to \omega\pi^0}(s)}{\Gamma(\omega \to \pi^0\gamma)}\frac{s^2 p_0^3}{\pi\alpha\rho_\omega}.$$

Data on $|F_{\omega\pi^0}(q^2)|^2$ at $1.05 \leqslant q^2 \leqslant 1.9$ GeV^2 are shown in Fig. 13 [these results were found from the values of $\sigma(e^+e^- \to \omega\pi^0)$ from Ref. 13].

In concluding this subsection of the paper we note that colliding e^+e^- beams have also been used to study the $K_L^0 - K_S^0$ transition form factor for the timelike region of momentum transfer, in the reaction[32] $e^+e^- \to K_L^0 K_S^0$.

c) Vector dominance and transition form factors

From the experiments discussed in the preceding sections emerged the first reasonably accurate quantitative information on the electromagnetic structure of neutral mesons. All these experimental results are summarized in Fig. 14 and also in Table III, where a comparison is made with the various theoretical models[33–47] which we will be examining in this section of the paper.

The general behavior of the transition form factors is in qualitative correspondence with the VDM. The slopes of all the form factors are positive (i.e., the form factors increase with increasing mass of the lepton pair) and are of the correct order of magnitude. The old data on the decays $\pi^0 \to e^+e^-\gamma$ and $\eta \to e^+e^-\gamma$, which lead to negative and very large slopes, have turned out to be erroneous, apparently because of (primarily) a limited statistical base, the lack of really "clean" experimental conditions, and the absence of radiative corrections.

A quantitative analysis shows, however, that while the form factor for the η meson in decay (2.15) agrees quite well with the VDM predictions within the experimental error, we observe significant discrepancies with this model for the conversion decays of the π^0 meson, (2.13), and of the ω meson (2.17).[6)] It is thus a natural first step to ask just what accuracy we should expect of the VDM predictions.

There is no basis to expect that this simple model would always give a good description of all physical processes. Point interactions between the photons and the quark fields may be manifested in several electromagnetic phenomena. A situation of this sort is known to occur at least at large momentum transfer (in the deep inelastic region), in the productin of lepton pairs with large effective masses, and in $\gamma\gamma$ collisions. There may be some specific contributions from individual quark diagrams which alter the naive estimates. We should also take into account vector states with large masses (a generalized VDM). There are well-known difficulties in comparing various physical processes with the VDM predictions, in connection with the extrapolation of data from $q^2 \approx m_V^2$ to $q^2 \approx 0$, etc. The general situation regarding the validity of vector dominance is thus not very satisfactory, and a specific analysis should be carried out in each individual case.

Such an analysis has been carried out[33] for the decays $P \to l^+l^-\gamma$. A study was made of the dispersion relations for the transition form factor

$$F_P(q^2; 0; m_P^2) = \frac{1}{\pi}\int_{s_0}^{\infty} ds \frac{\operatorname{Im} F_P(s; 0; m_P^2)}{s-q^2}. \qquad (2.34)$$

On the basis of data on e^+e^- annihilation to hadrons, the dispersion integral was broken up into two regions, a resonance region ($s < s_1 = 1.5$ GeV^2), approximated by the VDM, and a region of higher states ($s > s_1$), where QCD calculations can be used:

$$F_P(q^2; 0; m_P^2) = \underbrace{\frac{1}{\pi}\int_{s_0}^{s_1=1,5\,\text{GeV}^2} ds \left(\sum_V \; \begin{array}{c} l^- \quad l^+ \\ \diagdown \; \diagup \\ P \quad V \\ \diagup \\ \gamma \end{array}\right)}_{\text{resonant region}} + \frac{1}{\pi}\int_{s_1=1,5\,\text{GeV}^2}^{\infty} \frac{\operatorname{Im} F_P(s; 0; m_P^2)\, ds}{s-q^2}$$

$$= \left[\sum_V \frac{g_{PV\gamma}}{2g_{V\gamma}}\left(1-\frac{q^2}{m_V^2}\right)^{-1}\right]\left[\sum_V \frac{g_{PV\gamma}}{2g_{V\gamma}}\right]^{-1} + \frac{1\alpha_s}{3\sqrt{2}\pi}(\ldots) = \left[\sum_V \frac{g_{PV\gamma}}{2g_{V\gamma}}\left(1-\frac{q^2}{m_V^2}\right)^{-1}\right]\left[\sum_V \frac{g_{PV\gamma}}{2g_{V\gamma}}\right]^{-1}$$

$$+ O(1,5-5\%) \qquad (2.35)$$

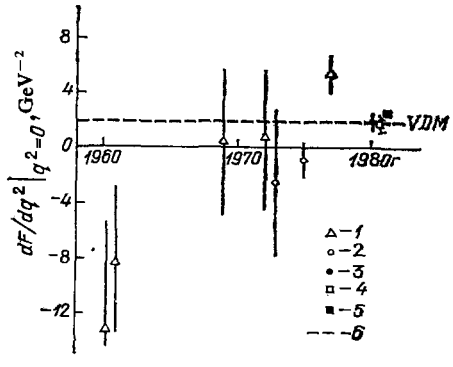

FIG. 14. Set of experimental data on the slopes of the electromagnetic transition form factors of neutral mesons, $[dF/dq^2]_{q^2\approx 0}$, GeV^{-2}. 1—The decay[22–25,10] $\pi^0 \to e^+e^-\gamma$; 2—the decay[27,28] $\eta \to e^+e^-\gamma$; 3—the decay[7] $\eta \to \mu^+\mu^-\gamma$; 4—the decay[8] $\eta' \to \mu^+\mu^-\gamma$; 5—the decay[9] $\omega \to \pi^0\mu^+\mu^-$; 6—prediction of the VDM for the slope of the form factor of the η meson, $[dF_\eta/dq^2]_{q^2\approx 0} = 1.8$ GeV^{-2} (the VDM predictions for the other slopes are very close to this value; see Table I).

TABLE III. Experimental data on the transition form factors and branching ratios for conversion decays and comparison with theoretical models.

	$\pi^0\to e^+e^-\gamma$ (2.13)		$\eta\to\mu^+\mu^-\gamma$ (2.15)		$\eta'\to\mu^+\mu^-\gamma$ (2.16)		$\omega\to\pi^0\mu^+\mu^-$ (2.17)	
	Br	b_{π^0},BeV^{-2}	Br	b_η,GeV^{-2}	Br	$b_{\eta'}$,GeV^{-2}	Br	$b_{\omega\pi^0}$,GeV^{-2}
Experimental data:	$(1.25\pm0.04\pm0.01)\cdot10^{-2}$	5.5 ± 1.6	$(3.1\pm0.4)\cdot10^{-4}$	1.9 ± 0.4	$(8.9\pm2.4)\cdot10^{-5}$	1.7 ± 0.4	$(9.6\pm2.3)\cdot10^{-5}$	2.4 ± 0.2
$\langle r^2_{AB}\rangle_{EM}$ (exptl.),10^{-13} cm	1.13 ± 0.16		0.67 ± 0.07		0.63 ± 0.07		0.75 ± 0.03	
Point particles (QED)	$1.19\cdot10^{-2}$	0	$2.1\cdot10^{-4}$	0	$3.4\cdot10^{-5}$	0	$5.0\cdot10^{-5}$	0
Vector dominance model	$1.21\cdot10^{-2}$	1.7	$(3.08\text{–}3.13)\cdot10^{-4}$	1.8	$(7.0\text{–}8.7)\cdot10^{-5}$	1.5	$8\cdot10^{-5}$	1.7
QCD corrections to VDM[33]	VDM holds within ~5–10% in the decays $P\to l^+l^-\gamma$.							
QCD asymptotic behavior[34–36]	The asymptotic behavior of the transition form factors for the $P\gamma\gamma$ vertex, which agrees with QCD, joins smoothly with the VDM at small momentum transfer.							
Dominance of triangle quark anomalies[37] (DTQA)	VDM should hold well for all these decays (better than on the average).							
Quarkloopmodel[38–42] (QLM), Q^2 duality	$b_p\approx(1/12)(1/m_q^2)$ (m_q is the effective mass of the quark). The Q^2 duality for the decays $P\to l^+l^-\gamma$ with a quark mass $m_u\approx m_d\approx250$ MeV and QLM leads to results similar to the VDM results.							
Baryon loop model[43] (BLM)	$b_p\approx(1/12)(1/m_N^2)\approx0.1$ GeV^{-2} (m_N is the mass of the nucleon). This model predicts very small slopes for the form factors, in contradiction with experimental data.							
Potential model[44]	$1.24\cdot10^{-2}$	~25	$3.4\cdot10^{-4}$	1.65	-	-		
Model of bound $q\bar{q}$ pairs with relativistic wave functions[45]	This model agrees with experimental data on the transition form factor in the decay $\eta\to\mu^+\mu^-\gamma$. For the decay $\pi^0\to e^+e^-\gamma$, this model is at odds with experiment, for the same reasons as for the potential model of Ref. 44 (the pole is at $q^2=m_p^2$)							
Nonlocal quark model (NQM)[46]	$\Gamma(\pi^0\to e^+e^-\gamma)=5.9\cdot10^{-2}$ eV	2.3	$\Gamma(\eta\to\mu^+\mu^-\gamma)=0.25$ eV	2.6	$\Gamma(\eta'\to\mu^+\mu^-\gamma)=17$ eV	1.6	$\Gamma(\omega\to\pi^0\mu^+\mu^-)=720$ eV	2.1
Bag model[47]							The form factor $\lvert F_{\omega\pi^0}(q^2)\rvert^2$ in the main q^2 region is several times smaller than that in the VDM (although it has the same slope $b_{\omega\pi^0}$ at very small values of q^2). There is a sharp contradiction with experiment.	

a) $b_{AB}=(dF_{AB}/dq^2)_{q^2\approx0}$ is the slope of the transition form factor.

b) $\sqrt{\langle r^2_{AB}\rangle_{EM}}=\sqrt{\frac{1}{6}b_{AB}}$ is the mean square "radius" of the structure of the A-B transition.

c) For decays (2.15)–(2.17), the errors also include systematic errors.[7–9] For the decay (2.13), the value b_{π^0} is given with statistical error only.[10]

d) In the NQM model[46], absolute values are given for the widths for conversion decays. The estimates of the branching ratios (relative probabilities) Br are

$$\mathrm{Br}(\pi^0\to e^+e^-\gamma)_{NQM}=7.4\cdot10^{-3},\quad \mathrm{Br}(\eta'\to\mu^+\mu^-\gamma)_{NQM}=6.1\cdot10^{-5},$$
$$\mathrm{Br}(\omega\to\pi^0\mu^+\mu^-)_{NQM}=7.3\cdot10^{-5},\quad \mathrm{Br}(\eta\to\mu^+\mu^-)_{NQM}=3.0\cdot10^{-4}$$

(the total widths are from the data of Ref. 48).

[since we have $\mathrm{Im}F_P(s) \sim \Sigma_V \delta(m_V^2 - s)$ in the resonance region]. Although the second integral is not estimated very accurately in QCD, it is important to note that this integral is very small in comparison with the first expression. It can thus be concluded that the corrections to vector dominance for the meson form factors in the decays $P \to l^+ l^- \gamma$ do not exceed 5–10%.

The QCD estimates thus show that the contribution of the higher-lying states to the transition form factor for the conversion decays of the type $P \to l^+ l^- \gamma$ is small and that the VDM should be quite successful. This interpretation is confirmed by the results of a study of the decay $\eta \to \mu^+ \mu^- \gamma$. However, data on the slope of the form factor of the π^0 meson, which differ from the predictions of the VDM by a factor of about three, present a well-known difficulty for this theory. There remains the unstudied question of how well the resonance region can be approximated by simple pole terms [see (2.35)]. The most important point to bear in mind here, however, is that measurements of the transition form factor of the π^0 meson pose difficulties, as mentioned above, and the corresponding experiments have to be repeated and refined.

We turn now to some possible mechanisms for the violation of the VDM in the decay $\omega \to \pi^0 \mu^+ \mu^-$, (2.17).

In Ref. 49 the transition $\omega\pi^0$ form factor was analyzed by a dispersion method, with allowance for intermediate $\pi\pi$ states ($\gamma_V \to \pi\pi \to \pi^0\omega$; see Fig. 15). It follows from the unitarity relation that the contribution from the amplitude of the reaction $\pi\pi \to \omega\pi^0$ must be taken into account in the expression for the form factor. According to the VDM, this amplitude is parametrized by the introduction of ρ poles in the s, t, and u channels, leading to some modification of the ρ-meson propagator in the transition form factor. Curve 2 in Fig. 11 shows the results of calculations carried out on the basis of this model. This curve agrees slightly better with the experimental points than does the prediction of the simple ρ-pole dominance, but the discrepancy with the experimental data is still significant.

If we assume that the reason why the $\omega\pi^0$ transition form factor increases more rapidly with increasing q^2 than the predictions based on the simple VDM is the contribution of heavier vector states V ("generalized vector dominance"), and if (for simplicity) we consider only the nearest state [which is apparently ρ' (1600)], then we would have

$$F_{\omega\pi^0}(q^2) \approx \frac{\frac{g_{\omega\pi\rho}}{2g_{\rho\gamma}}\left(1-\frac{q^2}{m_\rho^2}-i\frac{\Gamma_\rho}{m_\rho}\right)^{-1}+\frac{g_{\omega\pi\rho'}}{2g_{\rho'\gamma}}\left(1-\frac{q^2}{m_{\rho'}^2}-i\frac{\Gamma_{\rho'}}{m_{\rho'}}\right)^{-1}}{\frac{g_{\omega\pi\rho}}{2g_{\rho\gamma}}\left(1-i\frac{\Gamma_\rho}{m_\rho}\right)^{-1}+\frac{g_{\omega\pi\rho'}}{2g_{\rho'\gamma}}\left(1-i\frac{\Gamma_{\rho'}}{m_{\rho'}}\right)^{-1}}. \quad (2.36)$$

From a comparison with experimental data on the form factor $F_{\omega\pi^0}(q^2)$ in decay (2.17) we find a relation between interaction constants:

$$\frac{g_{\omega\pi\rho'}}{2g_{\rho'\gamma}} \approx -(0{,}5-0{,}7)\frac{g_{\omega\pi\rho}}{2g_{\rho\gamma}}. \quad (2.37)$$

In other words, the relative sign of the contributions of the heavy vector states must be negative. This conclusion agrees with the theoretical understanding based on an analysis of the asymptotic behavior of the π-meson form factors.[50] Accordingly, some of the deviations from the VDM predictions in the decay (2.17) can be explained, at least qualitatively, on the basis of heavier vector mesons. Unfortunately, a model of this sort slightly contradicts the data on $F(q^2)_{\omega\pi^0}$ at large values of q^2 found in the reaction $e^+e^- \to \omega\pi^0$ (Ref. 30; see Fig. 13 of the present paper). Accordingly, the behavior of the transition form factor $F_{\omega\pi^0}(q^2)$ requires further experimental and theoretical study.

d) Dynamic models for transition form factors

Up to this point, we have limited the theoretical discussion of the transition form factors to a purely phenomenological analysis based on the VDM and its possible generalizations. We would now like to turn to dynamic models for the structure of mesons, and we would like to attempt to relate the parameters of the transition form factors to characteristic properties of these models. We should bear in mind, however, that estimates of this sort for light mesons are frequently quite approximate and in fact are more in the realm of qualitative estimates.

1) Dominance of triangle quark anomalies[37]

The decays $P \to VV$ and $V \to PV$ of pseudoscalar and vector mesons (including the radiative decays $P \to 2\gamma$, $P \to V\gamma$, $V \to P\gamma$ and the corresponding conversion decays) were studied in Refs. 37 under the assumption that the amplitudes for these processes are dominated by triangle quark anomalies (the DTQA hypothesis). Analysis of the behavior of the transition form factors showed that incorporating only the anomalous part of the triangle diagram leads to a result for the decay amplitude which exactly reproduces the vector-dominance result. For the transition form factors we find, taking into account all vector mesons, the expression

$$F(q^2) = \sum_V C_V \left(1 - \frac{q^2}{m_V^2}\right)^{-1} \quad (2.38)$$

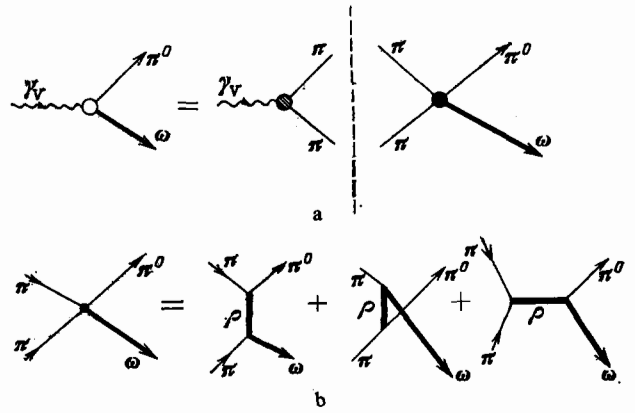

FIG. 15. Feynman diagrams for the transition form factor for the $\omega\pi^0$ vertex in the dispersion model of Ref. 49. a—Imaginary part of the form factor and the unitarity relation; b—parametrization of the amplitude for the reaction $\pi\pi \to \pi^0\omega$ through a ρ pole in the t, u, and s channels. In the model of Ref. 49, the real part of $F_{\omega\pi^0}$ is found from a dispersion relation.

$V = \rho, \omega, \varphi; \sum_V C_V = 1$ is the normalization). This expression agrees with (2.10). Ivanov and Shekhter[37] reach the qualitative conclusion that vector dominance should be quite successful in decays (2.13)–(2.17).

2) Quark triangle diagrams and Q^2 duality[38–42]

A very interesting approach to the analysis of transition form factors has been developed in Refs. 38–41. This approach is based on the concept of Q^2 duality, which had been formulated earlier[42] in an analysis of the total cross sections for e^+e^- annihilation. This duality establishes the equivalence of two different descriptions of low-energy phenomena: the purely phenomenological description based on vector dominance and the dynamic description based on the model of triangle quark loops (with the masses of the constituent quarks). According to the analysis of Refs. 38–41, the Q^2 duality agrees well with experimental data on the transition form factor of the η meson.[7] The transition form factors in the decays $P \to l^+ l^- \gamma$ are given by the following expression in the model of triangle quark loops with the phenomenological point interaction $\sim g\gamma_5$ between a pseudoscalar meson and the constituent quarks (Fig. 16a):

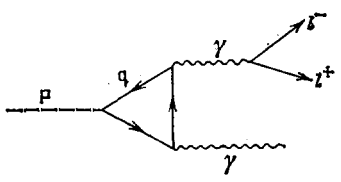

a

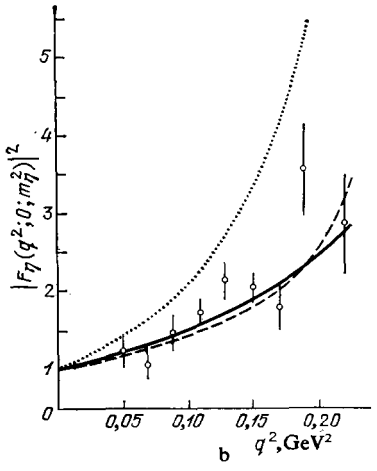

b

FIG. 16. Transition form factor of the η meson and Q^2 duality. a—Feynman diagram for decay (2.7) in the quark loop model; b—comparison of experimental data on the form factor of the η meson, $|F_\eta(q^2;0;m_\eta^2)|^2$, in decay (2.15) with predictions based on the triangle quark loop model. Circles—Experimental data of Ref. 7 (Fig. 9); solid line—predictions of the VDM; dashed line—results calculated in the quark loop model from (2.42), in the "soft-meson" approximation, for the η-meson wave function $|\eta\rangle = (1/\sqrt{3})(u\bar{u} + d\bar{d} - s\bar{s})$ (i.e., $\vartheta_P \approx -19°$) and for the quark masses $m_u = m_d = 0.25$ GeV and $m_s = 0.35$ GeV; dotted line—"double-counting" model in which the dependence on q^2 is found with allowance for both the masses of the quarks and the propagator of the vector meson.[38]

$$F(q^2;\ 0;\ m_P^2) = \frac{m_P^2}{m_P^2 - q^2}\left[1 - \left(\arcsin^2 \frac{\sqrt{q^2}}{2m_q}\right)\left(\arcsin^2 \frac{m_P}{2m_q}\right)^{-1}\right] \approx 1 + \frac{q^2}{m_P^2}\left[1 - \left(\frac{m_P}{2m_q}\right)^2 \left(\arcsin^2 \frac{m_P}{2m_q}\right)^{-1}\right] = 1 + \frac{q^2}{m_P^2}\left[1 - \frac{1}{1 + (1/6)(m_P/4m_q^2)}\right] \quad (2.39)$$

(we have initially considered the case of a quark loop with a single flavor and with a quark mass m_q). In the limit of "soft" mesons (i.e., $m_P \to 0$, $q^2 \neq 0$), which is frequently a rather good approximation, we easily find from (2.39)

$$F_P(q^2;\ 0;\ 0)_{(soft)} \approx \frac{4m_q^2}{q^2} \arcsin^2 \frac{\sqrt{q^2}}{2m_q} \approx 1 + \frac{q^2}{m_P^2} \cdot \frac{2}{6} \frac{m_P^2}{4m_q^2} = 1 + \frac{1}{12} \frac{1}{m_q^2} q^2. \quad (2.40)$$

For real neutral pseudoscalar mesons which are superpositions of quark loops with various flavors, the transition form factors are

$$F_P(q^2;\ 0;\ m_P^2) = \frac{1}{1 - (q^2/m_P^2)} \left\{ \sum_q \frac{g_{Pq\bar{q}}}{m_q} Q_q^2 \left[1 - \frac{\arcsin^2(\sqrt{q^2}/2m_q)}{\arcsin^2(m_P/2m_q)}\right]\right\} \times \left(\sum_q \frac{g_{Pq\bar{q}}}{m_q} Q_q^2\right)^{-1}, \quad (2.41)$$

$$F_P(q^2;\ 0;\ 0)_{(soft)} = \left(\sum_q \frac{4m_q^2}{q^2} \frac{g_{Pq\bar{q}} Q_q^2}{m_q} \arcsin^2 \frac{\sqrt{q^2}}{2m_q}\right)\left(\sum_q \frac{g_{Pq\bar{q}}}{m_q} Q_q^2\right)^{-1}, \quad (2.42)$$

where m_P is the mass of pseudoscalar meson P, m_q is the quark mass, $g_{Pq\bar{q}}$ are the constants of the coupling of the meson with the quark loops, and Q_q is the quark charge.

We now consider the η meson, represented as the quark superposition $\eta = (1/\sqrt{3})(u\bar{u} + d\bar{d} - s\bar{s})$. This superposition corresponds to a $\eta - \eta'$ mixing angle $\vartheta_P = -19°$, in good agreement with new experimental data on this angle.[51] Figure 16b shows transition form factors calculated for the decay $\eta \to \mu^+\mu^-\gamma$ in (2.15) in the VDM (solid line) and in the triangle-quark-loop model, from (2.42), for quark masses $m_u = m_d = 0.25$ GeV and $m_s = 0.35$ GeV (dashed line). The theoretical predictions agree well with each other and with the experimental data. These results depend rather weakly on the assumption made in the calculations in connection with the "soft-meson" approximation [i.e., the use of (2.42) instead of (2.41)] and the value selected for the mixing angle ϑ_D. These predictions provide good confirmation of the concept of Q^2 duality and show that the two approaches to the description of the form factor are equivalent and do not have to be used simultaneously. If we introduce a q^2 dependence due to the incorporation of both quark masses and a propagator of the vector meson (a "double count"), we find that this theoretical form factor has too steep a slope (the dashed curve in Fig. 16b), contradicting experimental data.

In connection with attempts to introduce a large characteristic mass in the physics of η mesons (Sec. 3), a model of baryon loops[43] has also been considered. To some extent, this model resurrects the old "prequark" approach to the electromagnetic decays of hadrons. In this model the photons are emitted directly by a virtual nucleon loop, and the following expressions is found for the slope of the form factor:

$$\frac{dF_P}{dq^2}\Big|_{q^2\approx 0} = \frac{1}{12}\frac{1}{m_N^2} \approx 0.1 \text{ GeV}^{-2} \qquad (2.43)$$

(m_N is the mass of the nucleon).

The baryon-loop model thus leads to a very small slope for the form factors in the decays $P\to l^+l^-\gamma$, completely at odds with the experimental results. The model is also completely unsatisfactory from the theoretical standpoint, since it is meaningless to talk about a point interaction of a photon and a baryon loop. At any rate, it should be noted that the electromagnetic transition form factors of the neutral mesons make it possible to sense the effective mass of the structural elements of hadrons, and this mass turns out to be much smaller than the masses of the baryons.

3) QCD asymptotic behavior of the transition form factors; vector dominance

It obviously cannot be claimed that the results calculated on the triangle quark diagrams discussed in the preceding subsection constitute an accurate quantitative description of the form factors of conversion decays. The concept of Q^2 duality developed in that subsection is more a qualitative than a quantitative model. Unfortunately, it is not possible to carry out more-systematic QCD calculations in the range of momentum transfer characteristic of $P\to l^+l^-\gamma$ decays. Such calculations can, however, be carried out at rather large values of q^2 (Ref. 34). As we will see below, this approach turns out to be useful in the analysis of $P\to l^+l^-$ decays, where the behavior of the form factors over the entire region of virtual momentum transfer is important. Babu and Ma[35] also took an asymptotic QCD approach to the analysis of the form factors in the decays $P\to l^+l^-\gamma$ and found that it was possible to establish an additional connection with vector dominance.

Following Babu and Ma,[35] we first consider the decay $\pi^0\to e^+e^-\gamma$. The asymptotic behavior of the transition form factor for this process is described at large q^2 in perturbative QCD by

$$|F_{\pi^0}(q^2)|_{q^2\to\infty} \to \frac{2f_\pi}{q^2\,|f(0;\,0;\,m_\pi^2)|}\,; \qquad (2.44)$$

here $f_{\pi^0} = 93$ MeV is the constant of the $\pi\to\mu\nu$ decay, and the quantity $f(0;0;m_\pi^2)$ is related to the probability for the $\pi^0\to\gamma\gamma$ decay,

$$\Gamma(\pi^0\to\gamma\gamma) = \frac{1}{4}\pi\alpha^2\,|f(0;\,0;\,m_\pi^2)|^2 m_\pi^3.$$

We thus find $|f(0;0;m_\pi^2)| = (2.76\pm 0.10)\cdot 10^{-4}$ MeV^{-1}. On the other hand, in the spirit of the approach involving vector dominance we would have $F_{\pi^0}(q^2) = [1-(q^2/m_{\text{eff}}^2)]^{-1}$. Comparing these two expressions in the limit $q^2\to\infty$ we find[7)]

$$m_{\text{eff}}^{(\pi^0)} = \sqrt{\frac{2f_\pi}{|f(0;0;m_\pi^2)|}} = 821\pm 15 \text{ MeV}. \qquad (2.45)$$

This result agrees with the value expected from VDM: $m_{\text{eff}}\approx m_\rho = 769$ MeV (although the experimental value is different, $m_{\text{eff}}^{(\pi^0)}\approx 430\pm 65$ MeV, as we mentioned earlier). For the η meson the asymptotic expression for the transition form factor in QCD is

$$|F_\eta(q^2)|_{q^2\to\infty} \to \frac{2f_\pi}{q^2\sqrt{3}}(\cos\vartheta_P - 2\sqrt{2}\sin\vartheta_P) \times |f(0;\,0;\,m_\eta^2)|^{-1}. \qquad (2.46)$$

Comparing with $F_\eta(q^2) = [1-(q^2/m_{\text{eff}}^2)]^{-1}$, we find[8)]

$$m_{\text{eff}}^{(\eta)} = \frac{2f_\pi}{\sqrt{3}}(\cos\vartheta_P - 2\sqrt{2}\sin\vartheta_P)\,|f(0;\,0;\,m_\eta^2)|^{-1} = 827\pm 35 \text{ MeV}. \qquad (2.47)$$

This value of m_{eff} agrees well with both the VDM and experimental data,[7] which yield $m_{\text{eff}}^{(\eta)} = 720\pm 90$ MeV [see (2.27)].

A QCD study has also been made of the behavior of $F_\pi(q_1^2;\,q_2^2;\,m_\pi^2)$ at large spacelike (and equal) values[36] $q_1^2 = q_2^2 = -Q^2$. The following expression was found:

$$\Phi(Q^2) \equiv F_{\pi^0}(-Q^2;\;-Q^2;\;0) = \frac{8\pi^2 f_\pi^2}{3Q^2}\left(1-\frac{5}{6}\frac{\alpha_s(Q^2)}{\pi}-\frac{1}{9}\frac{m_0^2}{Q^2}\right). \qquad (2.48)$$

It was also shown that the range of applicability of this expression corresponds to $Q^2>0.5$ GeV^2; here $\alpha_s(Q^2) = 4\pi/b\ln(Q^2/\Lambda^2)$ is the "constant" of the strong interaction in QCD, and the parameter values are $\Lambda\approx 0.1$ GeV and $m_0\approx 1$ GeV.

Figure 17 shows $\Phi(Q^2)$ as a function of Q^2 in the QCD approximation, (2.48), and in the VDM, $\Phi(Q^2)_{\text{VDM}} = [1-(q_1^2/m_\rho^2)]^{-1}[1-(q_2^2/m_\rho^2)]^{-1} = [1+(Q^2/m_\rho^2)]^{-2}$. We see from Fig. 17 that in the region $Q^2\approx 0.5$ GeV the two approximations converge.

These examples show that the asymptotic behavior of the transition form factors, which agrees with the predictions of QCD for large q^2, joins in a natural way with the

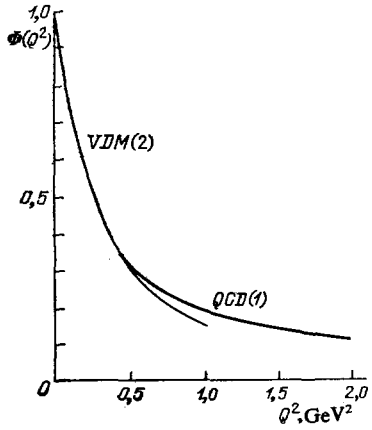

FIG. 17. $\Phi(Q^2) = F_{\pi^0}(-Q^2;\,-Q^2;0)$ as a function of Q^2 (Ref. 36). 1—QCD calculations [see (2.48)]; 2—VDM.

predictions of the VDM in the region of a small momentum transfer (as is characteristic of conversion decays).

4) Other dynamic models

We now consider some theoretical ideas which have been proposed for describing transition form factors in the conversion decays of mesons. Bergstrom and Snellman[44] studied a potential model in which the light mesons are described as bound states of quarks with effective masses ≈ 300 MeV. They carried out calculations in the lowest approximation in QCD, ignoring the gluon corrections. Since the form factor is normalized by the condition $F_P(q^2=0)=1$, there is the hope that the gluon corrections will not greatly change the results of these calculations. In the static limit the following expression was derived for the form factor of the η meson:

$$F_\eta(q^2) \approx \left(1-\frac{q^2}{m_P^2}\right)^{-1}\left(1-\frac{1}{2}\frac{q^2}{m_P^2}\right). \qquad (2.49)$$

Here we have $\mathrm{Br}(\eta\to\mu^+\mu^-\gamma)\approx 3.3\cdot 10^{-4}$, and the slope of the transition form factor is $(dF_\eta/dq^2)|_{q^2\approx 0}\approx (1/2)m_\eta^2 = 1.65\ \mathrm{GeV}^{-2}$. This result does not contradict experimental data, although, on the whole, the experimental results agree better with the VDM than with this potential model (Fig. 18).

An interesting qualitative feature of Bergstrom and Snellman's approach[44] is the idea that we should see significant deviations of the behavior of the transition form factors from the VDM predictions in conversion decays in the region of the maximum momentum transfer. As we see from Fig. 18, this region corresponds in the case of η mesons to values $q^2>0.26\ \mathrm{GeV}^2$, where we have no experimental data on the form factor $F_\eta(q^2)$ because of the limited statistical base. However, this conclusion does not have a really solid basis. The existence of a pole at m_P^2 (and not in the mass region of the vector mesons) is apparently a short-coming of this model, caused by approximations made in it. Specifically, the model must be drastically modified at the limiting values of q^2. We should also recall that although the potential models are a good approximation for nonrelativistic heavy quarkonia no claim is made that they give a quantitative description of light mesons. In particular, for π^0 mesons Bergstrom and Snellman's model[44] predicts completely incorrect results, in stark contradiction of experimental data on the form factor.

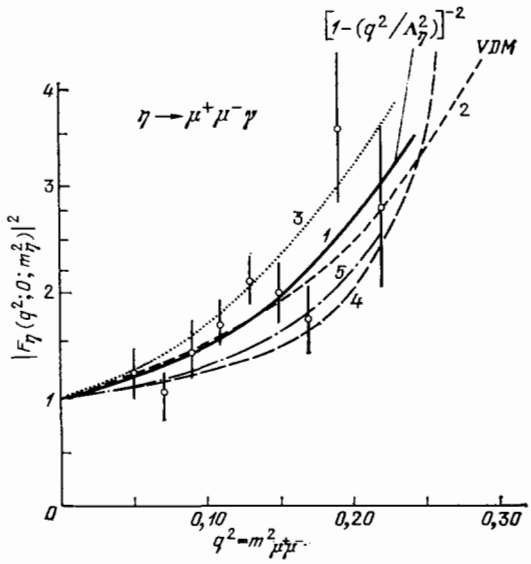

FIG. 18. Comparison of experimental data on the electromagnetic transition form factor of the η meson, $|F_\eta(q^2;0;m_\eta^2)|^2$, in decay (2.15) with the predictions of several theoretical models. Solid line 1—fit of experimental data by Eqs. (2.26) and (2.27); dashed line 2—VDM; dotted line 3—nonlocal quark model[46]; dashed line 4—potential model of Ref. 44; dot-dashed line 5—coupled-state model[45] (q^2 is given in units of GeV^2).

Kozlov *et al.*[45] calculated the transition form factors for the decays $P\to l^+l^-\gamma$ in a single-time formulation of quantum field theory, with relativistic wave functions for the bound quark-antiquark states, described by a quasipotential equation. They examined a one-gluon-exchange quasipotential and a blocking oscillator-type potential. They derived general expressions for the transition form factors for the decays $\pi^0\to e^+e^-\gamma$ and $\eta\to\mu^+\mu^-\gamma$. This model agrees with experimental data on the form factor of the η meson (Fig. 18). A distinctive feature of this model is the prediction of a possibly nonmonotonic behavior of the transition form factor with increasing q^2: At a very small momentum transfer, $q^2/m_P^2<0.1$, the form factor initially falls off slightly, dropping below unity, but later it begins to rise. The magnitude of this effect is governed by the shape of the wave function of a bound state of a quark and an antiquark, while the effect itself is a manifestation of the structure of the meson. Estimates show that this unusual behavior (if it actually occurs) of the transition form factor could in principle be observed in $\pi^0\to e^+e^-\gamma$ decays with a very large statistical base.

Efimov *et al.* and Dineĭkhan *et al.*[46] have described a nonlocal quark model (NQM) which is a self-consistent, relativistic, quantum-field bag model in which the quarks exist in a virtual state. The hadrons, which are bound quark formations, interact with each other through the exchange of quarks. In this model, with two adjustable parameters characterizing the quark fields, it is possible to find a unified description of many hadronic processes.

The decays $P\to l^+l^-\gamma$ and $\omega\to\pi^0 l^+l^-$ have been studied in the NQM, and expressions have been derived for the transition form factors and their slopes at $q^2\approx 0$. The results of the corresponding calculations are shown in Table III and Figs. 10, 11, and 18, where these results can be compared with experimental results and the predictions of other models.

We will also mention an attempt[47] to describe the transition form factor of the $\omega\pi^0$ vertex in the conversion decay $\omega\to\pi^0\mu^+\mu^-$ by means of a bag model. It turned out that in this model the square of the form factor is several times smaller than in the VDM and disagrees badly with experimental data[9] on $|F_{\omega\pi^0}(q^2)|^2$.

3. HIGHER-ORDER ELECTROMAGNETIC LEPTONIC DECAYS

In this section we consider higher-order electromagnetic decays of mesons in which a lepton pair is bound to a hadronic vertex by two virtual γ rays. The Feynman diagrams in Figs. 19 and 24 show examples of such decays. The

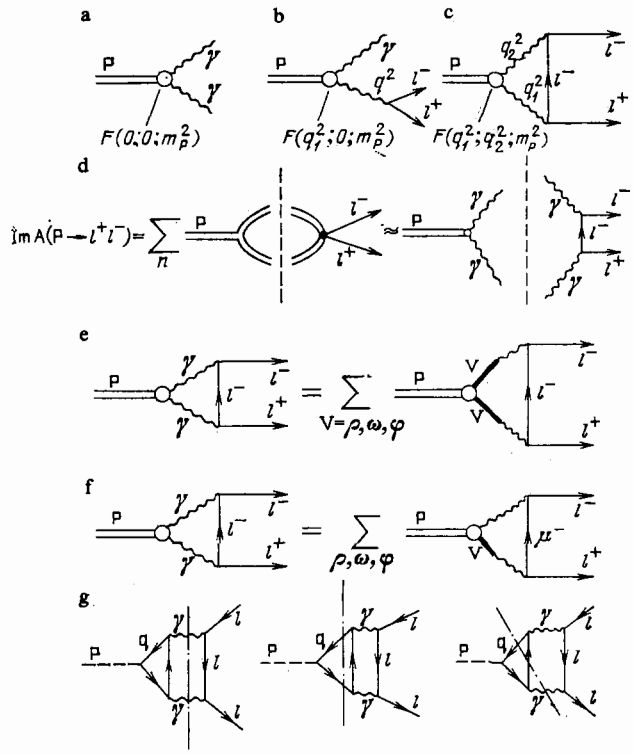

FIG. 19. Feynman diagrams for the electromagnetic decays of pseudoscalar mesons P. a—P→2γ; b—P→$l^+l^-\gamma$; c—P→l^+l^-; d—unitarity relation for P→l^+l^- decays; e—the decay P→l^+l^- in the VDM (both of the γ rays are coupled with the P through vector mesons; 3 in Table IV); f—the same, but only one γ ray is coupled with the P through vector mesons (4 in Table IV); g—with contribution of intermediate γγ, qq̄, and qq̄γ state in the dispersion relation for $X(m_P^2)$ (10 in Table IV).[40]

first process of this type which has been discovered and studied experimentally[52] is the decay $\eta\to\mu^+\mu^-$.

a) Leptonic decays of pseudoscalar mesons, P→l^+l^-

1) General description

The rare electromagnetic decays of pseudoscalar mesons,

$$P\to l^+l^-, \tag{3.1}$$

are fourth-order electromagnetic processes, intimately related to the radiative decays P→2γ, which occur in second order in the electromagnetic interaction, and with third-order conversion decays, P→$l^+l^-\gamma$ (Figs. 19a–19c). We recall that the matrix element of the Pγγ transition is given for real or virtual photons by

$$M(P\to\gamma\gamma)=4\pi i\alpha\zeta^{\mu\nu\delta\beta}q_{1\mu}q_{2\nu}e_{1\delta}e_{2\beta}f_{\gamma\gamma}F_P(q_1^2;\ q_2^2;\ P^2); \tag{3.2}$$

here q_1 and q_2 are the 4-momenta of the photons; $\varepsilon_{1\delta}$ and $\varepsilon_{2\beta}$ are their polarization vectors; and P is the 4-momentum of the pseudoscalar meson ($P=q_1+q_2$; we will be using the notation $P^2=s$). The coupling constant $f_{\gamma\gamma}$ is chosen to satisfy the form-factor normalization condition

$$F_P(0;\ 0;\ m_P^2)=1. \tag{3.3}$$

The branching ratio for decay (3.1) can be written

$$\mathrm{Br}(P\to l^+l^-)=\frac{\Gamma(P\to l^+l^-)}{\Gamma(P\to\text{all channels})}$$

$$=\mathrm{Br}(P\to\gamma\gamma)\cdot 2\alpha^2\xi^2\sqrt{1-4\xi^2}(|X|^2+|Y|^2)$$

$$=\mathrm{Br}(P\to\gamma\gamma)\cdot 2\alpha^2\xi^2\beta(|X|^2+|Y|^2); \tag{3.4}$$

here $\xi=m_l/m_P$; $\beta=\sqrt{1-4\xi^2}$; and Y and X are the imaginary (absorptive) and real (dispersive) parts of the dimensionless reduced amplitude of the decay P→l^+l^-.

From the unitarity relation which expresses the imaginary part of the amplitude Y in terms of the amplitude for the two-γ decay P→2γ (Fig. 19d) we have[14,53]

$$|Y|^2=(1-4\xi^2)^{-1}\ln^2\frac{1+\sqrt{1-4\xi^2}}{2\xi}=\frac{1}{4}\beta^{-2}\left(\ln\frac{1+\beta}{1-\beta}\right)^2. \tag{3.5}$$

We can now directly derive a lower limit on the branching ratio for the decay P→l^+l^-—the so-called unitary boundary or unitary limit:

$$\mathrm{Br}(\pi^0\to e^+e^-)\geqslant\mathrm{Br}(\pi^0\to e^+e^-)|_{\text{unit}}=4{,}75\cdot10^{-8}, \tag{3.6}$$

$$\mathrm{Br}(\eta\to\mu^+\mu^-)\geqslant\mathrm{Br}(\eta\to\mu^+\mu^-)|_{\text{unit}}$$

$$=\mathrm{Br}(\eta\to2\gamma)\cdot1.07\cdot10^{-5}=4.0\cdot10^{-6}, \tag{3.7}$$

$$\mathrm{Br}(\eta\to e^+e^-)\geqslant\mathrm{Br}(\eta\to e^+e^-)|_{\text{unit}}$$

$$=\mathrm{Br}(\eta\to2\gamma)\cdot4{,}5\cdot10^{-9}=1.7\cdot10^{-9}. \tag{3.8}$$

Because of the small mass m_e, electronic decays of the pseudoscalar mesons are strongly supressed by helicity conservation. For the total branching ratio for decay , we have the expression

$$\mathrm{Br}(P\to l^+l^-)=\mathrm{Br}(P\to l^+l^-)|_{\text{unit}}\left(1+\frac{|X|^2}{|Y|^2}\right). \tag{3.9}$$

The real part of the decay amplitude, X, diverges logarithmically for a point vertex, and calculations on this part of the amplitude must incorporate a cutoff, which is determined by the structure of the vertex, i.e., by the form factor $F_P(q_1^2;q_2^2;m_P^2)$.

The dispersive amplitude has been derived theoretically in several studies; the results are shown in systematic form in Table IV. In the first studies in this direction, the structure of the $P\gamma\gamma$ vertex was described by phenomenological structure functions or by form factors in the VDM, etc. More recently, however, we see a systematic approach to this problem,[35,40,54,59] based to a large extent on experimental data on the transition form factors in P→$l^+l^-\gamma$ decays, discussed in the preceding section.

The structure of the form factor $F_P(q_1^2;q_2^2;m_P^2)$ could, in fact, be studied experimentally in the spacelike region in experiments with colliding e^+e^- beams in the reactions $e^+e^-\to e^+e^-\gamma^*\gamma^*\to e^+e^-P$, i.e., in collisions in which the squares of the momentum transfers, q_1^2 and q_2^2, would be fixed in a detection of secondary e^+ and e^- particles (a double "tagging" of virtual photons). Unfortunately, no such data are available at this point, and apparently we cannot expect to see any in the near future because of the small values of the corresponding differential cross sections (especially at large values of q_1^2 and q_2^2).

It may, however, be required that the form factors

TABLE IV. Theoretical models for $P \to l^+ l^-$ decays.

Model	The form factor $F_P(q_1^2;q_2^2;s)$ for the $P\gamma\gamma$ vertex	Estimate of $\lvert X\rvert^2/\lvert Y\rvert^2$
1. Ref. 55 (1959).	A dispersion relation without a subtraction in the variable s is used for the estimate of X. A phenomenological cutoff is introduced for the form factor: $F_P(0,0,s) = \begin{cases} 1, & s<\Lambda^2, \\ 0, & s>\Lambda^2, \end{cases}$ The physical meaning of the cutoff parameter Λ is not determined.	$\lvert X\rvert^2/\lvert Y\rvert^2 \gtrsim 1$ at $\Lambda > 1.6$ GeV. The behavior of $\Gamma(\eta \to \mu^+\mu^-)/\Gamma(\eta \to 2\gamma)$ as a function of Λ is shown in Fig. 20.
2. Ref. 56 (1960).	The phenomenological form factor $F_P(q_1^2;q_2^2;m_P^2) = \Lambda^2/(\Lambda^2 - q_1^2 - q_2^2)$. It follows from data on $P \to l^+ l^- \gamma$ that we should have $\Lambda \approx m_\rho$.	$\lvert X\rvert^2/\lvert Y\rvert^2$ at $\Lambda \approx m_\rho$. The behavior of $\Gamma(\eta \to \mu^+\mu^-)/\Gamma(\eta \to 2\gamma)$ as a function of Λ is shown in Fig. 20. $\lvert X\rvert^2/\lvert Y\rvert^2 > 1$ at $\Lambda > 1.6$ GeV
3. Ref. 14 (1968). VDM. Both virtual γ rays are coupled with the P through vector mesons (Fig. 19e).	a) Model with a single vector meson with a mass m_V in the intermediate state: $F_P(q_1^2;\ q_2^2;\ m_P^2) = [1-(q_1^2/m_V^2)]^{-1}[1-(q_2^2/m_V^2)]^{-1}$. b) Vector dominance model (VDM): $F_P(q_1^2;\ q_2^2;\ m_P^2) = \sum_{V=\rho,\ \omega,\ \varphi} (g_{PV\gamma}/2g_{V\gamma}) \times \times [1-(q_1^2/m_V^2)]^{-1}[1-(q_2^2/m_V^2)]^{-1}\left[\sum_{V=\rho,\ \omega,\ \varphi}(g_{PV\gamma}/2g_{V\gamma})\right]^{-1}$. For the η meson in the SU_3 approximation with a mixing angle $\vartheta_P \approx 0$: $F_\eta(q_1^2;\ q_2^2;\ m_\eta^2) = \Big\{[1-(q_1^2/m_\rho^2)]^{-1}[1-(q_2^2/m_\rho^2)]^{-1} + \frac{1}{9}[1-(q_1^2/m_\omega^2)]^{-1}[1-(q_2^2/m_\omega^2)]^{-1} - \frac{4}{9}[1-(q_1^2/m_\varphi^2)]^{-1}[1-(q_2^2/m_\varphi^2)]^{-1}\Big\}[1+(1/9)-(4/9)]^{-1}$. The result depends weakly on the exact value of ϑ_P.	a) Model with a single vector meson: $\frac{\lvert X\rvert^2}{\lvert Y\rvert^2} = \begin{cases} 0{,}06, & V=\rho, \\ 0{,}09, & V=\omega, \\ 0{,}21, & V=\varphi. \end{cases}$ b) VDM: 1) For $\eta \to \mu^+\mu^-$, X (SU_3; VDM) $= (3/2)[X(\rho) + (1/9)X(\omega) - (4/9)X(\varphi)]$, $\lvert X\rvert^2/\lvert Y\rvert^2 \approx 10^{-2}$ (VDM; SU_3); 2) for $\pi^0 \to e^+e^-$, $\lvert X\rvert^2/\lvert Y\rvert^2 \approx 0{,}4$
4. Ref. 14 (1968). Only a single γ ray is coupled with the meson through a virtual vector meson (Fig. 19f).	a) In a model with a single vector meson for $F_P(q_1^2;\ q_2^2;\ m_P^2) = 0{,}5\{[1-(q_1^2/m_V^2)]^{-1} + [1-(q_2^2/m_V^2)]^{-1}\}$. b) In the VDM: $F_P(q_1^2;\ q_2^2;\ m_P^2) = \sum_{V=\rho,\ \omega,\ \varphi} 0{,}5\,(g_{PV\gamma}/2g_{V\gamma})\{[1-(q_1^2/m_V^2)]^{-1} + [1-(q_2^2/m_V^2)]^{-1}\}\left[\sum_{V=\rho,\ \omega,\ \varphi}(g_{PV\gamma}/2g_{V\gamma})\right]^{-1}$	This model leads to a form factor $P \to l^+ l^- \gamma F_P(q^2;0;m_P^2)$ with a slope $\frac{dF}{dq^2}\Big|_{q^2\approx 0} \approx \frac{1}{2}\frac{1}{m_\rho^2} \approx \frac{1}{2}\frac{dF}{dq^2}\Big|_{q^2\approx 0;\ \text{VDM}}$. This result contradicts experimental data on the decay $\eta \to \mu^+\mu^-\gamma$.
5. Ref. 43 (1972). Baryon loop model. Correction of Ref. 40 (1983).	This model leads to a form factor in the decay $P \to l^+ l^- \gamma$ of $F_P(q^2;0;m_P^2)$ with a slope $dF/dq^2\lvert_{q^2\approx 0} = (1/12)m_N^{-2} \approx 0.1\ \text{GeV}^{-2}$, which is in sharp contradiction with experimental data on $\eta \to \mu^+\mu^-\gamma$ and $\pi^0 \to e^+e^-\gamma$.	The decay[43] $\eta \to \mu^+\mu^-$[43]: $\lvert X\rvert^2/\lvert Y\rvert^2 \approx 2.4$. The decay $\pi^0 \to e^+e^-$: $\lvert X\rvert^2/\lvert Y\rvert^2 \approx 2.0$. In Ref. 40, where the numerical errors of the calculations of Ref. 43 were corrected, the following value was found in the same model: $\frac{\lvert X\rvert^2}{\lvert Y\rvert^2} = \begin{cases} 1{,}67, & \eta \to \mu^+\mu^-, \\ 0{,}08, & \pi^0 \to e^+e^- \end{cases}$

TABLE IV. (continued)

Model	The form factor $F_P(q_1^2;q_2^2;s)$ for the $P\gamma\gamma$ vertex	Estimate of $\lvert X\rvert^2/\lvert Y\rvert^2$
6. Ref. 37 (1980). The model of dominance of triangle quark anomalies.	It has been shown that for the form factors of pseudoscalar mesons in conversion decays this model is very similar to the VDM (Subsection 2d1). Calculations of X for $P\to l^+l^-$ decays have been carried out with the form function $F_\pi(q_1^2;\ q_2^2;\ m_{\pi^0}^2)=$ $=(1/2)\{[1-(q_1^2/m_\rho^2)]^{-1}[1-(q_2^2/m_\omega^2)]^{-1}+[1-(q_1^2/m_\omega^2)]^{-1}[1-(q_2^2/m_\rho^2)]^{-1}\},$ $F_\eta(q_1^2;\ q_2^2;\ m_\eta^2)=(9/2)\{[1-(q_1^2/m_\rho^2)]\ [1-(q_2^2/m_\rho^2)]\}^{-1}+$ $+(1/2)\{[1-(q_1^2/m_\omega^2)]\ [1-(q_2^2/m_\omega^2)]\}^{-1}\mp$ $\mp(\sqrt{2}/\lambda)\{[1-(q_1^2/m_\varphi^2)]\ [1-(q_2^2/m_\varphi^2)]\}^{-1}[5\mp(\sqrt{2}/\lambda)]^{-1}$ ($\lambda\approx 1.5$; the lower sign corresponds to η').	The results of the calculations are $\lvert X\rvert^2/\lvert Y\rvert^2=\begin{cases}0{,}29, & \pi^0\to e^+e^-,\\ 0{,}03, & \eta\to\mu^+\mu^-,\\ 2{,}05, & \eta\to e^+e^-,\\ 0{,}50, & \eta'\to\mu^+\mu^-,\\ 6{,}64, & \eta'\to e^+e^-\end{cases}$
7. Ref. 46 (1980,1981). Nonlocal quark model.	In the nonlocal quark model, the quarks exist in virtual states, and hadrons interact exclusively with quarks. The structure factors are determined by corresponding quark diagrams. The predictions for the form factors for conversion decays are quite close to the VDM results (Subsection 2d4).	The calculation results are $\lvert X\rvert^2/\lvert Y\rvert^2=\begin{cases}0{,}17, & \pi^0\to e^+e^-,\\ 0{,}98, & \eta\to\mu^+\mu^-,\\ 1{,}30, & \eta\to e^+e^-,\\ 1{,}0, & \eta'\to\mu^+\mu^-,\\ 4{,}62, & \eta'\to e^+e^-\end{cases}$
8. Ref. 35 (1982). Vector dominance and QCD (the model satisfies the QCD asymptotic limit).	$F_P(q_1^2;\ q_2^2;\ m_P^2)=[1-(q_1^2q_2^2/3m_{eff}^2Q^2)]\{[1-(q_1^2/m_{eff}^2)]\ [1-(q_2^2/m_{eff}^2)]\}^{-1},$ $Q^2=(1/2)(q_1-q_2)^2\approx(1/2)\left(q_1^2+q_2^2-\frac{1}{2}m_P^2\right);$ here the form factor for the decay $P\to l^+l^-\gamma$ is $F_P(q_1^2;\ 0;\ m_P^2)=[1-(q_1^2/m_{eff}^2)]^{-1}.$ According to the VDM and the QCD asymptotic predictions we have $m_{eff}=821\pm 15$ MeV for π^0 mesons and $m_{eff}=827\pm 35$ MeV for the η meson (m_{eff} is an effective mass in the VDM) (Subsection 2d3). $\lvert F_P(q_1^2\to\infty;\ q_2^2\to\infty;\ m_P^2)\rvert\approx\frac{m_{eff}^2}{3Q^2}$ { and satisfies the asymptotic predictions.	For $m_{eff}\approx m_\rho$, $\lvert X\rvert^2/\lvert Y\rvert^2=\begin{cases}0{,}32, & \pi^0\to e^+e^-,\\ 0{,}12, & \eta\to\mu^+\mu^-\end{cases}$
9. Ref. 57 (1982). Relativistic model of bound quark states.	In the static limit the form factor in this model is $F_P^{stat}(q_1^2;\ q_2^2;\ m_P^2)=m_P^2[m_P^2-q_1^2-q_2^2]^{-1}.$ The incorporation of higher-order corrections in QCD leads to $F_P(q_1^2;\ q_2^2;\ m_P^2)=m_P^2N(q_1^2,\ q_2^2)(m_P^2-q_1^2-q_2^2)^{-1}.$ The asymptotic behavior is $N(q_1^2\to\infty;0)=N(0;q_2^2\to\infty)=3/2$. $N(q^2,0)$ is given as a curve in that paper. The pole in $F_P(q_1^2;0;m_P^2)$ as $q^2\to m_P^2$ is a shortcoming of the bound-state model. A more accurate expression for the form factor is $F_P(q_1^2;\ q_2^2;\ m_P^2)=m_V^2(m_V^2-q_1^2-q_2^2)^{-1}$	$\lvert X\rvert^2/\lvert Y\rvert^2=\begin{cases}\approx 0, & \eta\to\mu^+\mu^-,\\ 2{,}8, & \eta\to e^+e^-,\\ 0{,}3, & \pi^0\to e^+e^-\end{cases}$

TABLE IV. (continued)

Model	The form factor $F_P(q_1^2;q_2^2;s)$ for the $P\gamma\gamma$ vertex	Estimate of $\lvert X\rvert^2/\lvert Y\rvert^2$
10. Ref. 40 (1983). Model of quark triangle diagrams with constituent quark masses.	An expression for $F_P(q^2;0;m_P^2)$ was derived, and the concept of Q^2 duality was confirmed (Subsection 2d2). A calculation of $X(m_P^2)$ wa carried out with the help of a dispersion relation without a subtraction: $$X(m_P^2)=\frac{1}{\pi}\,\mathrm{P}\int_0^\infty \frac{Y(t)\,dt}{t-m_P^2}$$ The intermediate states $\gamma\gamma$, $q\bar{q}$, and $q\bar{q}\gamma$ were taken into account (Fig. 19g). Direct calculations of the amplitude $A(P\to l^+l^-)$ for a quark loop in the soft-meson approximation ($m_P\to 0$) and by a numerical integration by the Monte Carlo method were also reported. It was shown that calculations in the soft meson approximation yield incorrect results for the decay $P\to l^+l^-$.	$\frac{\lvert X\rvert^2}{\lvert Y\rvert^2}=\begin{cases}0{,}23, & \pi^0\to e^+e^-,\\ 0{,}27, & \eta\to\mu^+\mu^-\end{cases}$
11. Refs. 39 and 62 (1983,1984). Quark loops with constituent quarks, Q^2 duality, dispersion relations. **Note:** The dimensionless amplitude R used in Refs. 39 and 62 is related to our amplitudes X and Y by $\mathrm{Re}\,R(s)=\pi X(s)$, $\mathrm{Im}\,R(s)=\pi Y(s)$	Calculation of the real part of the amplitude for the decay $\pi^0\to e^+e^-$ for triangle quark diagrams in various versions of the VDM (in accordance with Q^2 duality, for $m_V\approx 2m_q$). A dispersion relation in s with a subtraction was also used to estimate the real part of the amplitude: $$X(s)=X(0)+\frac{s}{\pi}\int_0^\infty ds'\,\frac{Y(s')}{(s'-s)\,s'}.$$ It was shown that $$X(m_P^2) = \underbrace{X(0)}_{\text{"Soft-meson" approximation}} + \underbrace{X^{(PL)}(m_P^2)}_{\text{Due to intermediate } \gamma\gamma \text{ states}} + \underbrace{rX^{(\Lambda)}(m_P^2)}_{\text{Due to intermediate states with hadrons}}\quad (0\leqslant r\leqslant 1).$$	For the decay $\pi^0\to e^+e^-$ we have $\lvert X\rvert^2/\lvert Y\rvert^2=0.26\pm 0.12$. Agreement with experiment on $\mathrm{Br}(\pi^0\to e^+e^-)$ [see (3.13) and (3.14)] requires choosing the value $\Lambda=4\cdot 10^5$ GeV. Such a cutoff parameter, however, leads to $\lvert X\rvert^2/\lvert Y\rvert^2\approx 700$, for the decay $\eta\to\mu^+\mu^-$ in sharp contradiction with experimental results. For the decay $\eta\to\mu^+\mu^-$, the model leads to the value $\lvert X\rvert^2/\lvert Y\rvert^2\approx 0.3\pm 0.3$ (for reasonable values of the cutoff parameter), in good agreement with experiment.
	For the decay $\pi^0\to e^+e^-$ we have $X(m_\pi^2)=(1/\pi)[3\ln(m_e/\Lambda)+\ln^2(m_e/m_\pi)]$ where Λ is a cutoff parameter ($m_e^2\ll m_\pi^2\ll\Lambda^2$). It was concluded that the real part of the amplitude depends on only the cutoff parameter Λ (the dependence is logarithmic), not on the detailed behavior of the form factor. For $\Lambda\approx m_\rho$ the result $X(m_\pi^2)=(1/\pi)(-22+31)=(1/\pi)(9\pm 2)$ was found, in agreement with the VDM predictions. For the real part of the amplitudes for the decays $\eta\to\mu^+\mu^-$ and $\eta\to e^+e^-$ the following relations were found: $$\left.\begin{aligned}X_{\eta\to\mu^+\mu^-}(m_\eta^2)-X_{\eta\to e^+e^-}(m_\eta^2)&=1/\pi\,[-30\pm 2],\\ X_{\pi^0\to e^+e^-}(m_\pi^2)-X_{\eta\to\mu^+\mu^-}(m_\eta^2)&=1/\pi\,[+12\pm 2],\end{aligned}\right\}\ \Lambda\approx m_\rho$$	

TABLE IV. (continued)

Model	The form factor $F_P(q_1^2;q_2^2;s)$ for the $P\gamma\gamma$ vertex	Estimate of $\lvert X\rvert^2/\lvert Y\rvert^2$
12. Ref. 58 (1982). Model with direct $P\gamma\gamma$ coupling. See also the 1984 discussion (Refs. 59 and 60).	Estimate of $X(s)$ for a model with direct $P\gamma\gamma$ coupling through a dispersion relation with a subtraction at $s=0$. The calculations were carried out under the assumption of a form factor $F(0;0,s)=1$ over the entire range of s (not only at $s=m_P^2$). In Ref. 59 this model was criticized (the authors did not agree with this criticism; see Ref. 60): It was shown that the assumptions made are equivalent to writing the form factor in the form $F_P(q_1^2;\ q_2^2;\ m_P^2)=m_P^4[m_P^4+q_1^4+q_2^4-2m_P(q_1^2+q_2^2)-2q_1^2q_2^2]^{-1}$. Then for $P\to l^+l^-\gamma$ we would have $F_P(q^2;0;m_P^2)=[1-q^2/m_P^2]^{-2}$; i.e., the form factor does not agree with the VDM c.: with experimental data. For large q^2 the result is $F_P\propto q^{-4}$, not q^{-2} as predicted by QCD.	The predictions of the model are $\lvert X\rvert^2/\lvert Y\rvert^2=\begin{cases}0{,}25-0{,}5, & \eta\to\mu^+\mu^-,\\ 4{,}3, & \eta\to e^+e^-,\\ 3{,}2, & \pi^0\to e^+e^-\end{cases}$
13. Ref. 61 (1984). Quark model, soft-meson approximation.	The soft-meson approximation ($s\to0$) was used to calculate X. The form factor in this case is $F_P(k^2;\ k^2;\ s=0)=\frac{2\alpha m_q^2}{\pi f_\pi}\int_0^1 x[k^2x(1-x)-m_q^2]^{-1}\,dx$ ($f_\pi=93$ MeV is the constant of the decay $\pi\to\mu\nu$; m_q is the mass of a constituent quark).	The results of the calculation are $\lvert X\rvert^2/\lvert Y\rvert^2=\begin{cases}1{,}7, & \eta\to\mu^+\mu^-,\\ 1, & \pi^0\to e^+e^-.\end{cases}$ The soft-meson approximation is apparently incorrect for an analysis of the decay[40] $P+l^+l^-$.
14. Ref. 41 (1984). Model of triangle quark loops.	$F_P(q_1^2;\ q_2^2;\ m_P^2)=$ $=-2m_q^2\int_0^1 d\beta_1\,d\beta_2\,\Theta(1-\beta_1-\beta_2)[\beta_1(1-\beta_1)m_P^2+\beta_2(1-\beta_2)q_2^2-$ $-2\beta_1\beta_2(p\cdot q_2)-m_q^2+i\varepsilon]^{-1}$ (here p is the 4 momentum of P). For the decay $P\to l^+l^-\gamma$ in the "soft-meson" limit, the result is $F_P(q^2;\ 0;\ 0)_{soft}\approx1+\frac{1}{12m_q^2}\cdot q^2$ (m_q is the mass of the quarks).	For the decay $\pi^0\to e^+e^-$
		m_q, MeV | $\lvert X\rvert^2/\lvert Y\rvert^2$
		100 | 0,52 150 | 0,39 200 | 0,32 250 | 0,28 300 | 0,24 350 | 0,21
15. Ref. 36 (1982,1984) QCD.	The behavior of $F_{\pi^0}(q_1^2;q_2^2;m_{\pi^0}^2)$ is determined in QCD for large spacelike, and equal, values $q_1^2=q_2^2=-Q^2$ [see (2.48)]. (см. (2.48))	For the decay $\pi^0\to e^+e^-$, the result is $\lvert X\rvert^2/\lvert Y\rvert^2\approx0{,}3$ (M. B. Voloshin).

$F_P(q_1^2; q_2^2; m_P^2)$ which are used in theoretical calculations of the real part (X) of the reduced amplitude for decay (3.1) satisfy the following conditions[59]:

1) At small values of q_1^2 (q_2^2), the form factors $F_P(q^2; 0; m_P^2)$ must be described by the VDM, as experiments have demonstrated; i.e., we must have $F_P(q_1^2; 0; m_P^2) = [1 - (q_1^2/\Lambda^2)]^{-1}$, where $\Lambda \approx m_\rho F_P(q_1^2; q_2^2, m_P^2) = \{[1 - (q_1^2/\Lambda^2)]\,[1 - (q_2^2/\Lambda^2)]\}^{-1}$.

2) At large q^2, as is shown by QCD calculations, the transition form factor must have the asymptotic form (Sections 2b and 3)

$$F_P(q_1^2; 0; m_P^2) \propto \frac{1}{q_1^2} \quad \text{or} \quad F_P[q^2; (r-q^2); m_P^2] \propto \frac{1}{q^2}.$$

These restrictions on the form factor $F_P(q_1^2; q_2^2; m_P^2)$ turn out to be sufficient to lead to quite reliable estimates of the dispersive amplitude X.

Analysis of the theoretical results in Table IV shows that under the conditions listed above the expected value of the ratio $|X|^2/|Y|^2$ for the decays

$$\eta \to \mu^+\mu^-, \tag{3.10}$$

$$\pi^0 \to e^+e^- \tag{3.11}$$

is quite small (only these decays have been studied experimentally; see Table IV, 3, 6–11, 14, and 15). This result means that the branching ratios for such decays should not substantially exceed the unitary limit.

We turn now to the experimental data. Table V shows the results of four experiments on the decays (3.10) and (3.11).

2) The decay $\eta \to \mu^+\mu^-$

The decay (3.10) was first detected in 1969 in an experiment by Hyams *et al.*[52] (1 in Table V), and the value of $\mathrm{Br}(\eta \to \mu^+\mu^-) = (2.2 \pm 0.8) \cdot 10^{-5}$ was found for its branching ratio. This value is several times the unitary limit in (3.7) and corresponds to the larger ratio $|X|^2/|Y|^2 \approx 2.5$–6.5. The only way to explain this dominant contribution of the dispersive amplitude X is to have a cutoff parameter of a few gigaelectronvolts for this logarithmically divergent amplitude (Fig. 20). As a rule, however, such large characteristic masses lead to very small slopes for the form factor for the conversion decay $\eta \to \mu^+\mu^-\gamma$, in direct contradiction of experiment. As we saw in Subsection 3a1, any reasonable assumptions regarding the structure of the $\eta\gamma\gamma$ vertex which are consistent with experiment lead to a small contribution of the real part of the amplitude, (3.10). Consequently, the experimental results of Ref. 52 pose serious difficulties in a theoretical interpretation.

New experiments on the $\eta \to \mu^+\mu^-$ have been carried out at the Serpukhov accelerator in experiments with the Lepton-G apparatus, and other rare electromagnetic decays have been studied simultaneously. As before, the source of the η mesons was the charge-exchange reaction $\pi^- p \to \eta n$.

In the processing of the data, there was a selection of events with two hard muons formed in the target of the apparatus and not accompanied by additional charged-particle tracks from the interaction vertex. A further requirement is that there be no γ or hadron showers in the hodoscopic γ spectrometer of the Lepton apparatus (Fig. 6); i.e., the γ spectrometer was used in an "anticoincidence" mode with a low energy threshold (0.5 GeV for a γ ray).

For the final analysis, events with kinematics corresponding to the exclusive reaction $\pi^- p \to \mu^+\mu^- n$ were selected, and the effective-mass spectrum of the muon pairs was studied. As can be seen from Fig. 21, this spectrum is dominated by events of the reaction

$$\left\{\begin{array}{l}\pi^- p \to \rho(\omega)\, n. \\ \qquad\quad \big\downarrow \\ \qquad\quad \to \mu^+\mu^-\end{array}\right.$$

In the region of the η meson in the spectrum there is a peak corresponding to the decay $\eta \to \mu^+\mu^-$. The width of this peak is determined by the instrumental resolution, and its mass is 551 ± 4 MeV, in agreement with the tabulated value for the η meson. The peak contains 27 ± 8 events of decay (3.10) and emerges more than five standard deviations above the background.

A study of events of the more intense decay $\eta \to \mu^+\mu^-\gamma$ in (2.15) (see Subsection 2b1) was carried out at the same time as the study of process (3.10) on the same apparatus. It thus became possible to study in detail the background conditions for the detection of decay (3.10) and to measure its branching ratio reliably. The background below the η-meson peak is physical in nature and can be described in the VDM as a direct process in which muon pairs are produced.The decay $\eta \to \mu^+\mu^-\gamma$ (and also in-flight decays of π mesons accompanied by the production of muons) is of negligible importance.

To determine the relative probability for the decay $\nu \to \mu^+\mu^-$, the data were normalized to the number of events (2.15) detected simultaneously, and the quantity $\mathrm{Br}(\eta \to \mu^+\mu^-\gamma) = (3.1) \pm 0.4) \cdot 10^{-4}$, determined earlier, was used. The efficiency of the apparatus for decays (2.10) and (2.15) was calculated by the Monte Carlo method. The branching ratio for decay (3.10) found as the result is

$$\mathrm{Br}(\eta \to \mu^+\mu^-) = (6{,}5 \pm 2{,}1) \cdot 10^{-6}. \tag{3.12}$$

This value is smaller than the value found previously by a factor of three. In comparing the results of the two experiments on the decay $\eta \to \mu^+\mu^-$ one should bear in mind that the Serpukhov data are more reliable since they are normalized on the basis of the well-known branching ratio for the conversion decay $\eta \to \mu^+\mu^-\gamma$ (Subsection 2b1). Furthermore, in the experiments carried out at CERN to measure the branching ratio for the decay[63] $\rho \to \mu^+\mu^-$, at the same time and on the same apparatus as for the study of decay (3.10), the branching ratio $\mathrm{Br}(\rho \to \mu^+\mu^-) = (0.97 \pm 0.31) \cdot 10^{-4}$ was found. This value is substantially higher than the worldwide average[48] $\mathrm{Br}(\rho \to l^+l^-) = (0.428 \pm 0.045) \cdot 10^{-4}$. There is accordingly the suggestion that there is a general systematic error in the normalization in the experiments of Refs. 52 and 63 which leads to overestimates of the branching ratios for the decays $M \to l^+l^-$.

The result in (3.12) can thus be used as a final value for the relative probability for the decay $\eta \to \mu^+\mu^-$. This value

TABLE V. Experimental studies of the decays $P \to l^+ l^-$

Study and particular decay	Summary of experimental apparatus	Number of events of the decay $P \to l^+ l^-$	Br ($P \to l^+ l^-$)
1. [52] (1969), CERN, $\eta \to \mu^+\mu^-$	Magnetic spectrometer with optical spark chambers; detection of charged particles; identification of muons and measurement of their momentum.	18±6	$(2{,}2\pm0{,}8)\cdot10^{-5}$
2. Ref. 54 (1980), IHEP, Serpukhov, $\eta \to \mu^+\mu^-$	Lepton-G apparatus (Subsection 2b1; Fig. 6). Magnetic spectrometer with proportional and wire spark chambers and a multichannel γ spectrometer. Detection of muons and γ rays and measurement of their energies. The same apparatus which was used for the study of the decay $\eta \to \mu^+\mu^-$ was used at the same time for a study of the decay $\eta \to \mu^+\mu^-\gamma$, making it possible to achieve good background conditions and to achieve a reliable normalization of the branching ratio for the decay.	27±8 (Fig. 21)	$(6{,}5\pm2{,}1)\cdot10^{-6}$
3. [64] (1978), CERN, $\pi^0 \to e^+e^-$	Magnetic spectrometer with wire spark chambers and gas-filled Cherenkov counters for identifying electrons and measuring their momenta (Subsection 2b1; Fig. 5). The source of the "tagged" π^0 mesons is the in-flight decay $K^+ \to \pi^+\pi^0$. The same apparatus which was used for the study of $\pi^0 \to e^+e^-$ was used for a simultaneous study of the intense decay $\pi^0 \to e^+e^-\gamma$. The results are important for studying the background conditions.	~6 (см. Fig. 22)	$\left(2{,}23\ {}^{+2{,}4}_{-1{,}1}\right)\cdot10^{-7}$ (the indicated errors are at the 90% confidence level)
4. [65] (1982), Los Alamos, $\pi^0 \to e^+e^-$	Magnetic spectrometer with proportional chambers and gas-filled Cherenkov counters for identifying electrons and measuring their momenta. The experiments were carried out in an intense π^--meson beam at the LAMPF meson factory. The $\pi^0 \to e^+e^-$ events detected are poorly distinguishable above the background.	59±21 (см. Fig. 23)	$(1{,}8\pm0{,}6\pm0{,}3)\cdot10^{-7}$

of the branching ratio agrees well with the theoretical estimates mentioned earlier and it completely eliminates the "problem" of the large real part of the amplitude for decay (3.10).

3) The decay $\pi^0 \to e^+e^-$

The branching ratios for the electromagnetic decays of pseudoscalar mesons accompanied by the emission of an electron pair are (as mentioned earlier) strongly suppressed in comparison with those for muon decays because of helicity conservation. Because of the very small branching ratio for the electron decays, the best change for success is in a search for decays (3.11), since very intense sources of π^0 mesons are available, especially at meson factories at low energies. At this writing, two such experiments have been carried out (3 and 4 in Table V).

In the first,[64] carried out at CERN at the same time as a study of the conversion decays $\pi^0 \to e^+e^-\gamma$ (Subsection 2b1), the source of the tagged π^0 mesons consisted of the decays

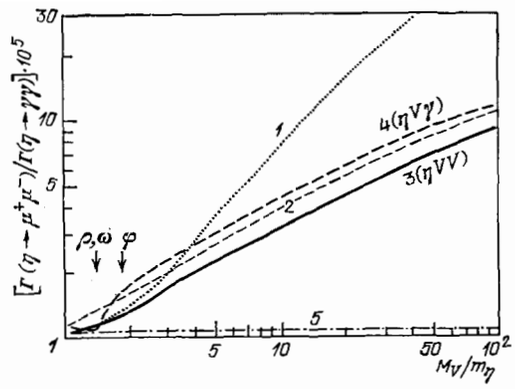

FIG. 20. The ratio of decay probabilities $\Gamma(\eta\to\mu^+\mu)/\Gamma(\eta\to2\gamma)^{-1}$ as a function of the mass of the vector meson in models of the VDM type or of the characteristic mass (the cutoff parameter) in the phenomenological models.[14] 1—Model of Ref. 55 (1 in Table IV); 2—model of Ref. 56 (2 in Table IV); 3—model of Ref. 14 (3 in Table IV); 4—mode of Ref. 14 (4 in Table IV); 5—unitary limit, (3.7).

$K^+\to\pi^+\pi^0$ decays

$\longrightarrow e^+e^-(\gamma)$

in flight. We recall that the γ rays are not detected directly but are instead reconstructed from the kinematics. Figure 22a shows the hard part of the spectrum of electron pairs, for $0.9\leqslant(x=m_{e^+e^-}/m_{\pi^0})\leqslant1.06$, in a two-dimensional plot in which the quantity plotted along the second coordinate is the energy found from the "γ ray" from the decay $K^+\to\pi^+ + (\pi^0\to e^+e^-\gamma)$ as the result of a fit. A comparison of the measured spectrum with the results of Monte Carlo calculations (Fig. 22, b–d) for the process $\pi^0\to e^+e^-$ and for the most important background processes, $\pi^0\to e^+e^-\gamma$ and $K^+\to\pi^+e^+e^-$, led the authors to the conclusion that there is an excess of 5.6 events above the expected background (1.4 events) in the region $0.94\leqslant x\leqslant1.02$ (i.e., at the mass of the π^0 meson). This excess was interpreted as a manifestation of the decay $\pi^0\to e^+e^-$. The estimated branching ratio is

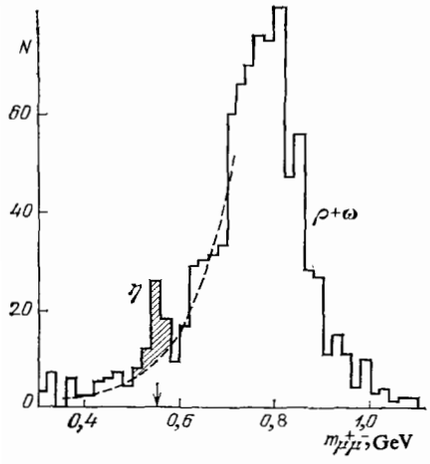

FIG. 21. Mass spectrum of $\mu^+\mu^-$ pairs in reaction (2.24) (Ref. 54). The arrow shows the tabulated mass of the η meson. Dashed curve—result of a fit of the background; N—number of events per 20-MeV mass interval; hatched peak—the decay $\eta\to\mu^+\mu^-$.

$$\mathrm{Br}(\pi^0\to e^+e^-)=(2{,}23^{+2{,}4}_{-1{,}1})\cdot10^{-7}, \tag{3.13}$$

where the errors are purely statistical and correspond to a 90% confidence level. This value is about two standard deviations above the unitary limit, (3.6).

Another experiment on decay (3.11) was carried out at the LAMPF meson factory (at Los Alamos).[65] The source of the π^0 mesons was the charge-exchange reaction $\pi^-p\to\pi^0n$ at a primary-pion energy of 300 MeV. The decay $\pi^0\to e^+e^-$ was detected by means of a wide-aperture spectrometer with proportional chambers and gas-filled Cherenkov counters for identifying electrons. The total flux of π^- mesons passed through the target of the apparatus during the experiment was $2.4\cdot10^{13}$ particles. Events of the type $\pi^-p\to e^+e^-$ with a total energy >290 MeV of the two electrons were selected for analysis. There turned out to be 1330 candidate events of this type; the effective-mass spectrum of the e^+e^- pairs was determined for them. This spectrum is due primarily to the background from conversion decays $\pi^0\to e^+e^-\gamma$, from decays $\pi^0\to2\gamma$ with an external conversion of the γ rays in the target material, and also random coincidences. A careful analysis of the results and a comparison with Monte Carlo calculations led the authors to assert that they observed an excess above the background in the mass region of the π^0 meson, corresponding to 59 ± 29 events of the decay $\pi^0\to e^+e^-$ (Fig. 23). The value found for the branching ratio as a result is

$$\mathrm{Br}(\pi^0\to e^+e^-)=[1.8\pm0.6\ (\text{statist.})\pm0.3\ (\text{syst.})]\cdot10^{-7}. \tag{3.14}$$

This value agrees with the results of the earlier experiment[64] and is almost four times the unitary limit, (3.6). Such a large branching ratio is difficult to explain on the basis of the existing theory for decay (3.11) (Table IV), but it must be kept in mind that the experimental data are not yet really convincing and require further refinement. For this reason, the results in (3.13) and (3.14) should be regarded as more in the way of upper limits on $\mathrm{Br}(\pi^0\to e^+e^-)$, corresponding to a value $\leqslant(4\text{–}5)\cdot10^{-7}$ (90% confidence level).

Nevertheless, hypotheses have already been advanced which have the large branching ratio for $\pi^0\to e^+e^-$ resulting from new anomalous interactions.[57] Analysis shows that the possible contribution of neutral weak currents is at the level $\mathrm{Br}(\pi^0\to e^+e^-)\sim10^{-15}$, while mechanisms involving the exchange of an axion lead to $\mathrm{Br}(\pi^0\to e^+e^-)_{\text{axion}}\approx5\cdot10^{-11}$. Consequently, if the large value for $\mathrm{Be}(\pi^0\to e^+e^-)$ is confirmed by new experiments, it might be worthwhile to look for manifestations of more-exotic mechanisms here. At present, at least one more experiment on the decay $\pi^0\to e^+e^-$ is being carried out at CERN.[66] So far, the preliminary results of this experiment lead to only an upper limit on the probability for decay (3.11), and this upper limit is comparable to that from the earlier studies.[64,65]

Resolution in terms of the effective mass of the electron pair is of decisive importance for a reliable identification of the decay $\pi^0\to e^+e^-$. Accordingly, it is very important to minimize repeated scattering in the target which serves as the source of the π^0 mesons. Future experiments in intense

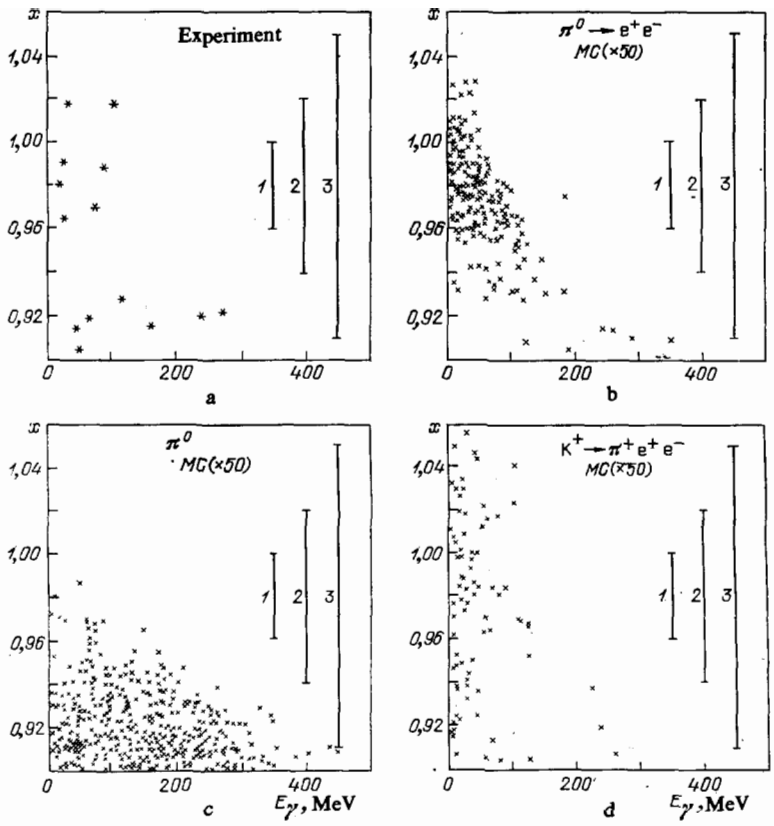

FIG. 22. Searches for the decay $\pi^0 \to e^+e^-$ in an analysis of the process[64] $K^+ \to \pi^+\pi^0; \pi^0 \to e^+e^- + (\gamma)$. The γ ray is not detected and is instead determined for a kinematic fit. Consequently, $\pi^0 \to e^+e^-$ events correspond to a very low energy of the "γ ray." a—Two-dimensional plot in the plane of $x = m_{e^+e^-}/m_{\pi^0}$ and E_γ of candidate $\pi^0 \to e^+e^-$ events; b–d—the same, for distributions expected according to Monte Carlo (MC) calculations for the following processes: b) $K^+ \to \pi^+\pi^0, \pi^0 \to e^+e^-$; c) $K^+ \to \pi^+\pi^0, \pi^0 \to e^+e^-\gamma$; d) $K^+ \to \pi^+e^+e^-$ (with a statistical base 50 times greater than the number of events in the experimental distribution). 1–3: Various regions of the selection of events in x.

beams of $K^\pm$ and K^0 mesons (tagged π^0 mesons produced in in-flight K decays) are extremely promising. There is the hope that new experiments will make it possible to resolve the question of the existence of decay (3.11) and the question of its branching ratio in the near future.

b) Searches for the decays $P' \to Pl^+l^-$

The pseudoscalar-meson decays

$$P' \to Pl^+l^- \qquad (3.15)$$

may occur in the two-photon approximation according to the diagram in Fig. 24a (the single-photon process, in Fig. 24d, is forbidden by charge parity conservation). The expected width for decay (3.15) depends on the structure of the $P' \to P\gamma\gamma$ vertex. This structure can be described by, for example, the VDM (Fig. 24b)[67] or the related model of $\delta(\varepsilon)$ dominance (Fig. 24c). It should be kept in mind that for this second mechanism, because of the conservation of the helicity of the leptons, decays accompanied by the emission of an electron pair are suppressed further, by about two orders of magnitude, with respect to muon decays.[67]

The two-photon mechanism leads to very small widths for decays of the type in (3.15) ($Br \ll 10^{-6}$), making these processes extremely sensitive to manifestations of various exotic mechanisms.

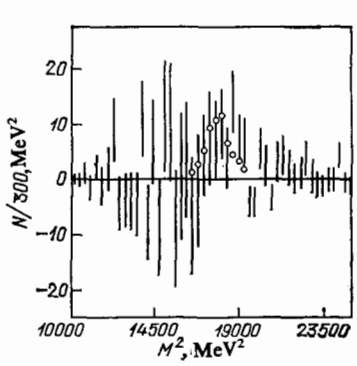

FIG. 23. Effective-mass spectrum of the e^+e^- system in the mass region of the π^0 meson in Ref. 65. The quantity plotted here is the difference between the experimental data and the background curve. The circles show a "signal" corresponding to 59 events of the decay $\pi^0 \to e^+e^-$.

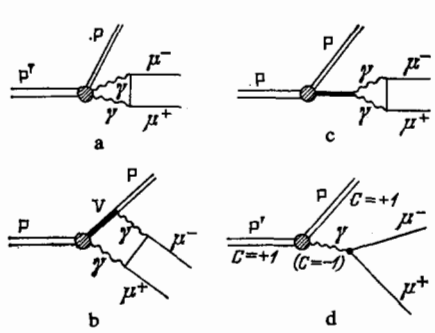

FIG. 24. Feynman diagrams for the decays $P' \to P\mu^+\mu^-$. a—General form of the two-γ vertex; b—two-γ vertex in the VDN (V is a vector meson); c—two-γ vertex in the $\delta(\varepsilon)$ dominance model; d—one-γ process with C-parity breaking (because of the negative C parity of the γ ray).

For example if light Higgs particles H ($J^P = 0^+$) exist, they could be observed in P′→P transitions from decay into a muon pair:

$$\begin{array}{l} P' \to PH \\ \qquad\quad \big\lfloor\!\!\longrightarrow \mu^+\mu^- \cdot \end{array} \qquad (3.16)$$

Another example of an exotic decay mechanism for (3.15) is a possible violation of charge parity in electromagnetic interactions (as in the model of Ref. 68). In this case, the decays of interest might occur in the single-photon approximation (Fig. 24d), with a probability far higher than the two–photon estimates.

Searches for decays of the type in (3.15) have been carried out in many experimental studies with a wide variety of methods—ranging from the first, relatively insensitive experiments in bubble chambers to complicated electronic experiments with high selectivity and luminosity. In none of these experiments have electromagnetic transitions between pseudoscalar states, accompanied by the emission of a lepton pair, been discovered. Upper limits have been established on the branching ratios for these decays. The data from the most sensitive experiments are listed in Table VI.

To illustrate the results we consider the searches for the decays

$$\eta \to \pi^0\mu^+\mu^-, \qquad (3.17)$$

$$\eta' \to \pi^0\mu^+\mu^-, \qquad (3.18)$$

$$\eta' \to \eta\mu^+\mu^-, \qquad (3.19)$$

carried out in 1980 on the Lepton-G apparatus at Serpukhov,[69] at the same time as a study of several other rare electromagnetic decays, mentioned earlier (Subsections 2b1 and 3a2). As before, the sources of the η and η' mesons were the binary reactions $\pi^-p \to \eta(\eta')n$, in (2.21). During the experiment, about $5 \cdot 10^{11}$ π^- mesons passed through the target; this number corresponds to the production of $2 \cdot 10^7$ η and 10^7 η' mesons in binary processes (2.21).

In the processing of the experimental data, events corresponding to the exclusive reaction $\pi^-p \to \mu^+\mu^-\gamma\gamma n$ were selected. Figure 25 shows a two–dimensional distribution of these events in the effective masses of the $\mu^+\mu^-\gamma\gamma$–and $\gamma\gamma$–systems ($m_{\mu^+\mu^-\gamma\gamma}$ and $m_{\gamma\gamma}$). The concentration of events in the regions $m_{\mu^+\mu^-\gamma\gamma} \approx m_\omega$ and $m_{\gamma\gamma} \approx m_{\pi^0}$ corresponds to the decay $\omega \to \pi^0\mu^+\mu^-$.

In region III, which corresponds to decay (3.19) (the resolution of the apparatus is taken into account), there is only a single event. In regions I and II, for (3.17) and (3.18), there is no significant excess of events above a uniform background.

Decays (3.17)–(3.19) were thus not observed in this experiment. The high sensitivity of this experiment makes it possible to set low upper limits on the branching ratios for these decays, providing an improvement of several orders of magnitude over the previous limits (Table VI).

As mentioned earlier, decays (3.17)–(3.19) can be used to search for light Higgs bosons. Athough the existing theories of weak interactions give preference to heavy Higgs bosons it should be noted that there is no theoretical lower limit on the mass of the Higgs bosons in models containing several doublets of these bosons. Consequently, searches for Higgs particles should be carried out over the entire possible mass range.

The theoretical situation has been examined in detail elsewhere.[70,71] A characteristic feature of the interaction of Higgs bosons with fermion fields is an increase in the coupling constant with the mass of the fermions. For this reason, at masses which are not too large ($M_H \lesssim (.5\ \text{GeV})$ the Higgs particles decay primarily into a muon pair:

$$H \to \mu^+\mu^-. \qquad (3.20)$$

Light Higgs bosons would most naturally be sought in processes of the type

$$\begin{array}{l} \eta' \to \pi^0 H \\ \qquad\quad \big\lfloor\!\!\longrightarrow \mu^+\mu^-, \end{array} \qquad (3.21)$$

$$\begin{array}{l} \to \eta H \\ \qquad \big\lfloor\!\!\longrightarrow \mu^+\mu^-. \end{array} \qquad (3.22)$$

Decays (3.21) and (3.22) and semiweak and should have branching ratios $\text{Br} \sim 10^{-5}$.

Figure 26 shows the results which have been calculated on the differential probabilities for decay (3.22) along with the corresponding experimental limiting estimates.[69] We see from this figure that experiments make is possible to rule out the existence of Higgs bosons over the entire interval[91] kinematically accessible in decay (3.22), i.e., for

$$2m_\mu < M_H < 409\ \text{MeV}. \qquad (3.23)$$

The data on decay (3.21) are not sensitive enough for a search for Higgs particles.

4. CONCLUSION

Recent experiments have provided the first opportunity to obtain important information on the electromagnetic structure of neutral mesons. On the one hand, the results of these studies confirm our general understanding of the important role played by vector mesons in mechanisms for interactions with virtual photons; on the other hand, they reveal some new details of this process, which require more detailed experimental and theoretical analysis. Let us consider briefly the outlook for further research on the electromagnetic structure of neutral mesons.

Experiments on the decays $\pi^0 \to e^+e^-\gamma$ can be carried out at meson factories, where a substantial increase in the statistical base is possible. However, there remain the difficulties associated with radiative corrections and radiative processes in the material of the apparatus. In this connection there is the interesting possibility of studying the conversion decays of π^0 mesons produced in very thin film targets as the inner proton beam of an accelerator passes through them repeatedly (I wish to thank L. L. Nemenov for calling my attention to this possibility). A careful experimental study of $\pi^0 \to e^+e^-\gamma$ decays would be very desirable for deciding whether there are significant violations of vector dominance in this process, contradicting the QCD analysis.[33] Another

TABLE VI. Upper limits on the branching ratios for the electromagnetic decays $P' \to P l^+ l^-$

Study	Apparatus	Upper limits on the branching ratio $Br(P' \to P l^+ l^-)$ (90% confidence level)					
		$\eta' \to \pi^0 e^+ e^-$	$\eta' \to \pi^+ \pi^0 \mu^-$	$\eta' \to \pi^0 e^+ e^-$	$\eta' \to \pi^+ \pi^0 \mu^-$	$\eta' \to \eta e^+ e^-$	$\eta' \to \pi^+ \pi^- \mu^-$
1.[69] (1980)	Lepton-G apparatus (Subsection 2b1). Automated spectrometer with detection of charged particles and γ rays; measurement of their momenta and energies; identification of muons.	—	$5 \cdot 10^{-6}$	—	$6 \cdot 10^{-5}$	—	$1{,}5 \cdot 10^{-5}$
2.[72] (1976)	Xenon 30-liter bubble chamber.	$1{,}6 \cdot 10^{-4}$	—	$0{,}8 \cdot 10^{-3}$	—	—	—
3.[73] (1975)	Spectrometer with optical spark chambers; identification of electrons by gas-filled Cherenkov counters.	$4{,}5 \cdot 10^{-5}$	—	—	—	—	—
4.[74] (1968)	Apparatus with spark chambers and iron filters to measure the range of the muons and for their identification.	—	$5 \cdot 10^{-4}$	—	—	—	—
5.[75] (1965)	Liquid-hydrogen bubble chamber.	—	—	$1{,}3 \cdot 10^{-2}$	—	$1{,}1 \cdot 10^{-2}$	—

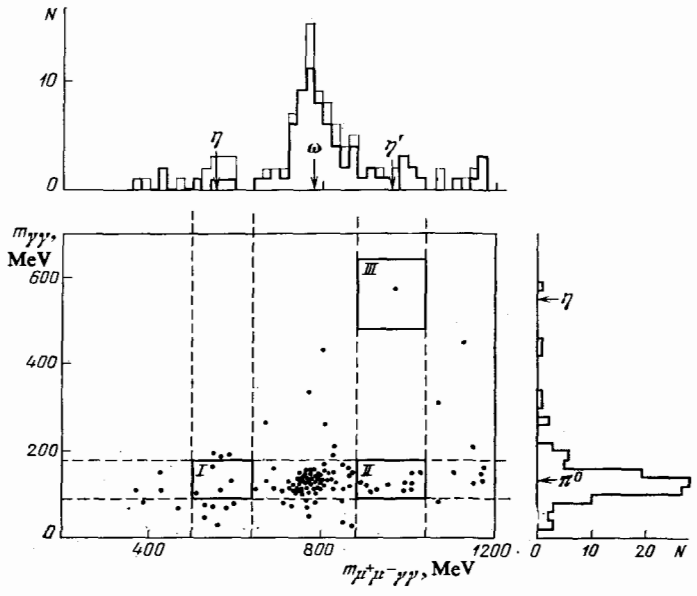

FIG. 25. Two-dimensional distribution of $\pi^- p \to \mu^+ \mu^- \gamma\gamma n$ events in the effective masses of the $\mu^+\mu^-\gamma\gamma$ and $\gamma\gamma$ systems ($E_\mu > 4.5$ GeV; $E_\gamma > 1.4$ GeV).[69] Regions I–III—Decays (3.17)–(3.19), with allowance for the experimental resolution; light histogram—all events; heavy histogram—events with the selection criterion $m_{\gamma\gamma} \approx m_{\pi^0}$. The arrows show the tabulated masses of the mesons.

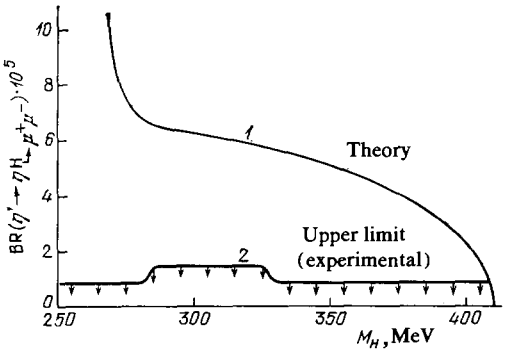

FIG. 26. Data on the decay $\eta' \to \eta H$; $H \to \mu^+\mu^-$ (Ref. 69). 1—Theoretical prediction of the branching ratio for the decay; 2—experimental upper limits (90% confidence level).

very interesting possibility is to test the theoretical predictions[45] of a possible nonmonotonic behavior of the transition form factor $F_{\pi^0}(q^2)$ in the region of small momentum transfer.

A new experiment on the decay $\pi^0 \to e^+e^-\gamma$ is presently being carried out at the TRIUMF meson factory with an apparatus including two total-absorption spectrometers with proportional chambers and large NaI(Tl) crystal detectors.[76] The expected accuracy of the measurement of the slope parameters of the transition form factor $b_{\pi^0} = (dF_{\pi^0}/dq^2)|_{q^2\approx 0}$ in this experiment is $\Delta b_{\pi^0} \approx 1$ GeV^{-2} (i.e., better by a factor of 1.6 than in the last experiment[10]).

It would be difficult to make any further progress in experiments on the conversion decays of η, η', and ω mesons like those which have been carried out on the Lepton apparatus at Serpukhov. We recall that the total flux of π^- mesons in the experiments which have already been carried out has been $\sim 5 \cdot 10^{11}$ particles, and the efficiency of the apparatus with respect to the various processes has been in the range 10–20%. It would thus not be possible to increase greatly the luminosity of the experiments, and the statistical base for the study of decays (2.15)–(2.17) could be increased by a factor of only a few units at the cost of an extremely large effort. However, even such a modest increase in the statistical base would be desirable, especially for the decays of the η' and ω mesons.

In experiments carried out in the Lepton apparatus the source of the mesons under study were the binary charge-exchange processes in (2.21) at large energies, where the cross sections are several microbarns. In inclusive processes at the same energies, in contrast, the cross sections for the production of these mesons are one or two orders of magnitude larger than the cross section for reaction (2.21). In this case, however, the background conditions for the experiments are substantially worse, and the softer spectrum of product particles requires a significant increase in the dimensions of the apparatus in order to maintain the same efficiency.

Roughly the same increase in the cross sections for binary reactions leading to meson production can be achieved at small initial energies of the π^- mesons (1–2 GeV). At these energies, however, high-luminosity experiments will also require a very large apparatus. Furthermore, at low energies there are the difficulties of identifying the secondary particles (muons and γ rays); there is an intensified background from in-flight $\pi \to \mu$ decays; etc. There is the complicated problem of organizing a good triggering of the apparatus.

There is the possibility of seeking compromise solutions: using certain semi-inclusive processes, optimizing the dimensions of the apparatus and the energy of the primary beam, etc. However, in view of the many difficulties listed above, we could hardly expect any rapid progress on the form factors of particles in experiments of this sort.

The branching ratios expected for several meson conversion decays are listed in Table VII. It should be notd that some of these branching ratios turn out to be quite large and could be studied experimentally, although it should be recalled (Subsection 2a) that an optimum study of transition form factors should focus on decays accompanied by the emission of muon pairs, for which the branching ratios are 10–20 times smaller than the branching ratios for electron decays. On the other hand, it should be kept in mind that study of decays of the type $A_2 \to \omega e^+e^-$ or $f \to \rho e^+e^-$ at small values of the effective mass of the lepton pairs [i.e., as $q^2 \to (2m_e)^2 \approx 0$] may prove useful for determining the constants $f_{A_2\omega}(0)$, etc., and thus for determining the widths of the corresponding radiative decays under background conditions more favorable than those in experiments carried out to detect these decays directly.

Calculations on radiative transitions for tensor mesons (and for other nonets with nonzero orbital quantum number L in the $q\bar{q}$ system) and more complicated and less definite than those for the decays $V \to P\gamma$ and $P \to V\gamma$, since they require allowance for electromagnetic processes with a different multipolarity. The theoretical estimates based on various models disagree with each other by more than an order of magnitude. As mentioned earlier, the radiative decays of mesons have not been studied at all adequately. These results are of major interest for reaching an understanding of the quark structure of mesons and of the mechanisms for the mixing of various quark and gluon states, for determining the mixing angles in nonets, and for resolving several other important questions. Consequently, further experimental work in this direction would be very valuable and looks very promising.

The electromagnetic structure of neutral mesons can be studied in completely different experiments: in various reactions in colliding e^+e^- beams (Subsection 2b2). So far, experiments of this sort have yielded only very preliminary results, and we can expect many interesting new results in the near future.

Returning to the research on the leptonic decays of mesons, we should point out that recent experimental results on higher-order electromagnetic leptonic processes have eliminated the previous difficulty in explaining the large branching ratio for the decay $\eta \to \mu^+\mu^-$, i.e., have eliminated the problem of the large real part of the amplitude for this process. The new data agree well with the results on the electromagnetic structure of the η meson extracted from an analysis of the decay $\eta \to \mu^+\mu^-\gamma$.

TABLE VII. Branching ratios for some conversion decays of mesons

Decay channel	$\Gamma(A \to Bl^+l^-)/\Gamma(A \to B+\gamma)$	$\frac{Br(A \to Bl^+l^-)}{\Gamma(A \to Bl^+l^-)/\Gamma(A \to anything)}$	Notes
$\varphi \to \eta+\mu^+\mu^-$	$4{,}7\cdot10^{-4}$	$9{,}4\cdot10^{-6}$	(Ref. 15). The conversion decays of the φ mesons have a low branching ratio. Furthermore, the sources of φ mesons are not very intense. One of the best sources is the resonant production $e^+e^- \to \varphi$. Several events of the decay $\varphi \to \eta e^+e^-$ were detected in experiments with a neutral detector at the Institute of Nuclear Physics, Novosibirsk, and its branching ratio was determined[30]: $Br(\varphi \to \eta e^+e^-) = (1{,}3^{+0{,}8}_{-0{,}6})\cdot10^{-4}$ [sic]
$\varphi \to \eta+e^+e^-$	$8{,}5\cdot10^{-3}$	$1{,}7\cdot10^{-4}$	
$\varphi \to \pi^0+\mu^+\mu^-$	$9{,}0\cdot10^{-4}$	$1{,}2\cdot10^{-6}$	
$\varphi \to \pi^0+e^+e^-$	$9{,}01\cdot10^{-3}$	$1{,}3\cdot10^{-5}$	
$\eta' \to \rho^0+e^+e^-$	$6{,}8\cdot10^{-3}$	$2{,}1\cdot10^{-3}$	
$A_2^0 \to \omega+e^+e^-$	$1{,}2\cdot10^{-2}$	$1{,}2\cdot10^{-3}$	(Ref. 77). The radiative widths of the tensor mesons were estimated to be very large in this study: 5–10% of their total widths. In other studies,[78] the predicted widths are an order of magnitude smaller (so that the branching ratios for the conversion decays are also smaller).
$A_2^0 \to \omega+\mu^+\mu^-$	$2\cdot10^{-3}$	$2\cdot10^{-4}$	
$f \to \rho^0+e^+e^-$	$1\cdot10^{-2}$	$5\cdot10^{-4}$	

The first experiments on the decay $\pi^0 \to e^+e^-$ are still too preliminary to support a serious discussion of whether the branching ratio for this process is significantly higher than the corresponding unitary limit. Here we need new and more accurate results.

Several experiments have yielded very low limits on the widths for other leptonic electromagnetic decays of pseudoscalar mesons which are of considerable interest for searches for various exotic processses. Further progress in this direction is very desirable but will be confronted with some serious practical difficulties, associated with both an increase in the luminosity and sensitivity of the experiments and an improvement in the background conditions.

In conclusion I would like to express the hope that the next stage in the development of experimental research on the leptonic decays of light mesons will involve weak interactions. Of foremost interest here are the conversion decays $K_L^0 \to e^+e^-\gamma$ and $K_L^0 \to \mu^+\mu^-\gamma$. So far, only a few events of this type have been detected, and we have only very crude estimates of their branching ratios: $Br(K_L^0 \to e^+e^-\gamma) = (1.7 \pm 0.9)\cdot10^{-5}$ and $Br(K_L^0 \to \mu^+\mu^-\gamma) = 2.8 \pm 2.8 \cdot 10^{-7}$ (Ref. 79). A detailed study of these processes would be very interesting both for learning about the electromagnetic structure of the K^0 particles and for resolving certain specific questions of the theory of weak interactions, in particular, the role played by "penguin" diagrams in nonleptonic weak decays.[80] A thorough study of the decays $K_L^0 \to \mu^+\mu^-$ and $\eta \to \mu^+\mu^-$ may yield information on the mechanisms for higher-order weak decays and may make it possible to test GIM compensation for flavor-changing neutral weak currents, with allowance for the t-quark contribution.[81] Finally, it may someday become possible to take up the study of not only the electromagnetic decays but also the weak decays of π^0 and η mesons,[82] although at the moment it is difficult to see how and when these dreams could ever come true.

I wish to thank A. I. Vaĭnshteĭn, M. B. Voloshin, G. V. Efimov, A. M. Zaĭtsev, V. I. Zakharov, B. L. Ioffe, A. E. Kaloshin, V. P. Kubarovskiĭ, V. F. Obraztsov, L. B. Okun', Yu. D. Prokoshkin, V. A. Khoze, and M. A. Shifman for useful discussions.

[1)]The transition form factors could in principle also be studied in the spacelike region in the interactions of neutral particles with electrons: $Ae^- \to Be^-$. However, because of the very short lifetime of most of these particles, an experiment of this sort has been carried out only for long-lived K_L^0 mesons: $K_L^0 e^- \to K_S^0 e^-$.

[2)]For decay (2.7) we again denote the transition form factor by $F_P(q^2;0)$ or $F_P(q^2;0;m_P^2)$ in order to emphasize that the second γ ray is on the mass shell.

[3)]With increasing primary energy, the cross sections for exclusive reactions (2.21) decrease, but the efficiency of the apparatus in the detection of meson decays (2.15)–(2.17) increases. Furthermore, the identification of the secondary particles (muons and γ rays) becomes more reliable, and the background due to in-flight $\pi \to \mu$ decays decreases. For this reason, the choice of primary energy has been the result of a compromise to maximize the sensitivity of the experiment.

[4)]The error in this preliminary normalization determines the difference of the factor K (see Fig. 9) from unity.

[5)]In expression (2.33) for the form factor of the η' meson, which was used in Ref. 29 (Fig. 12b), the small contribution of ω and φ mesons is ignored. The more accurate expression is $F_{\eta'}(q^2;0;m_{\eta'}^2) \approx [1 + (0.88Q^2/m_\rho^2)]^{-1}$ [see (2.10)–(2.12) and Table I].

[6)]The range of momentum transfer in the decay $\omega \to \pi^0\mu^+\mu^-$ is slightly higher than in the decay $\eta \to \mu^+\mu^-\gamma$, and it is primarily in this harder part of the dimuon spectrum that we see the deviations from the VDM.

[7)]Current algebra predicts the well-known result $|f(0;0;m_\pi^2)| \approx |f(0;0;0)| \approx \alpha/(\pi f_\pi \cdot 4\pi\alpha) = 1/(4\pi^2 f_\pi)$ for the anomalous triangle quark diagram. We then find $|F_\pi \cdot (q^2)| \underset{q^2\to\infty}{\to} (8\pi^2/f_\pi^2)/q^2$ and $m_{\text{eff}}^{(\pi^0)} = \sqrt{2\pi}\, f_\pi = 2\sqrt{2\pi} \cdot 93$ MeV $= 826$ MeV.

[8)]For $|f(0;0;m_\eta^2)| = (2.84 \pm 0.24) \cdot 10^{-4}$ MeV^{-1} and $\vartheta_P = -17.6°$ (Ref. 51).

[9)]Accepting certain theoretical concepts regarding the properties of Higgs bosons (for greater details see Ref. 69 and the bibliography there).

[1]B. L. Ioffe, Rapporterskiĭ doklad na XXII Mezhdunarodnoĭ konferentsii po fizike chastits vysokikh énergiĭ (Rapporteur Talk, Twenty-Second International Conference on the Physics of High-energy Particles), Leipzig, 1984.

[2]P. J. O'Donnell, Rev. Mod. Phys. **53**, 673 (1981); Can. J. Phys. **55**, 1301 (1977).

[3]Y. I. Azimov, Preprint LNPI-819, Leningrad Institute of Nuclear Physics, Leningrad, 1982.

[4]A. T. Filippov, Usp. Fiz. Nauk **137**, 201 (1982) [Sov. Phys. Usp. **25**, 371 (1982)]; Pis'ma Zh. Eksp. Teor. Fiz. **32**, 74 (1980) [JETP Lett. **32**, 69 (1980)].

[5]T. Ohshima, Phys. Rev. **D22**, 707 (1980).

[6]V. M. Budnev *et al.*, Phys. Rep. **C15**, 183 (1975); J. B. Dainton, in: Proceedings of the International Europhysics Conference on High Energy Physics, Brighton, UK, 20–27 July 1983; Rutherford Laboratory Preprint RL 83-103-1983; H. Kolanoski, Preprint Bonn HE-84-06, Bonn, 1984 (to be published in Springer Tracts in Modern Physics).

[7]Yu. B. Bushnin *et al.*, Yad. Fiz. **28**, 1507 (1978) [Sov. J. Nucl. Phys. **28**, 775 (1978)]; Phys. Lett. **B79**, 147 (1978); V. A. Viktorov *et al.*, Yad. Fiz. **32**, 998 (1980) [Sov. J. Nucl. Phys. **32**, 516 (1980)]; Phys. Lett. **B94**, 548 (1980).

[8]V. A. Viktorov *et al.*, Pis'ma Zh. Eksp. Teor. Fiz. **30**, 387 (1979) [JETP Lett. **30**, 359 (1979)]; Phys. Lett. **B88**, 379 (1979); V. A. Viktorov *et al.*, Yad. Fiz. **32**, 1005 (1980) [Sov. J. Nucl. Phys. **32**, 520 (1980)].

[9]V. A. Viktorov *et al.*, Yad. Fiz. **29**, 1513 (1979) [Sov. J. Nucl. Phys. **29**, 777 (1979); Phys. Lett. **B84**, 143 (1979); V. A. Viktorov *et al.*, Pis'ma Zh. Eksp. Teor. Fiz. **33**, 239 (1981) [JETP Lett. **33**, 228 (1981)]; Phys. Lett. **B102**, 296 (1981).

[10]J. Fisher *et al.*, Phys. Lett. **B73**, 359 (1978).

[11]R. H. Dalitz, Proc. Phys. Soc. **A64**, 667 (1951).

[12]N. M. Kroll and W. Wada, Phys. Rev. **98**, 1355 (1955).

[13]C. Jarlskog and H. Pilkuhn, Nucl. Phys. **B1**, 264 (1967).

[14]C. Quigg and J. D. Jackson, Preprint UCRL-18487, 1968.

[15]C. H. Lai and C. Quigg, Preprint FNAL FN-296 2000.000, Batavia, 1976.

[16]V. F. Obraztsov, Preprint IFVÉ 79-115, Institute of High-Energy Physics, Serpukhov, 1979.

[17]L. G. Landsberg, Élektromagnitnye raspady legkikh mezonov. Teksty lektsiĭ (Electromagnetic Decays of Light Mesons. Lecture Texts), MIFI, Moscow, 1981.

[18]M. P. Rekalo, Ukr, Fiz. Zh. **28**, 1308 (1983); Preprint KhFTI-83-12, Khar'kov Physicotechnical Institute, 1983.

[19]M. Gell-Mann and F. Zachariasen, Phys. Rev. **124**, 953 (1961).

[20]R. P. Feynman, Photo-Hadron Interactions, Benjamin, New York, 1972 (Russ. Transl. Mir, Moscow, 1975); J. Sakurai, Currents and Mesons, Univ. Chicago Press, 1969 (Russ. Transl. Atomizdat, Moscow, 1972); T. H.Bauer *et al.*, Rev. Mod. Phys. **50**, 261 (1978).

[21]V. M. Budnev and V. A. Karnakov, Pis'ma Zh. Eksp. Teor. Fiz. **29**, 439 (1979) [JETP Lett. **29**, 398 (1979)].

[22]N. P. Samios *et al.*, Phys. Rev. **121**, 275 (1961).

[23]H. Kobrak *et al.*, Nuovo Cimento **20**, 1115 (1961).

[24]S. Devons *et al.*, Phys. Rev. **184**, 1356 (1969).

[25]J. Burger, NEVIS-190, Thesis, 1972.

[26]N. A. Schardt *et al.*, Phys. Rev. **D23**, 639 (1981).

[27]A. Kotlewski, Preprint Columbia Univ., New York, 1973.

[28]M. R. Jane *et al.*, Phys. Lett. **B59**, 103 (1975).

[29]Ch. Berger *et al.* (PLUTO Collaboration), Phys. Lett. **B142**, 125 (1984).

[30]V. P. Druzhinin *et al.*, Preprint INP 84-93, Institute of Nuclear Physics, Novosibirsk, 1984.

[31]N. M. Budnev and A. I. Orlov, Pis'ma Zh. Eksp. Teor. Fiz. **32**, 390 (1980) [JETP Lett. **32**, 365 (1980)].

[32]P. M. Ivanov *et al.*, Pis'ma Zh. Eksp.Teor. Fiz. **36**, 91 (1982) [JETP Lett. **36**, 112 (1982)]; F. Mang *et al.*, Phys. Lett. **B99**, 261 (1981).

[33]M. A. Shifman and M. I. Vysotsky, Z. Phys. **C10**, 131 (1981).

[34]G. P. Lepage and S. J. Brodsky, Phys. Rev. **D22**, 2157 (1980).

[35]K. S. Babu and E. Ma, Phys. Lett. **B119**, 449 (1982).

[36]M. B. Voloshin, Preprint ITEF-8, Institute of Theoretical and Experimental Physics, Moscow, 1982; see also V. A. Novikov *et al.*, Nucl. Phys. **B237**, 525 (1984).

[37]A. I. Ivanov and V. M. Shekhter, Yad. Fiz. **31**, 530 (1980) [Sov. J. Nucl. Phys. **31**, 275 (1980)]; **32**, 796 (1980) [Sov. J. Nucl. Phys. **32**, 410 (1980)].

[38]A. Bramon and E. Masso, Phys. Lett. **B104**, 311 (1981).

[39]L. Bergstrom *et al.*, Phys. Lett. **B126**, 117 (1983).

[40]Ll. Ametller *et al.*, Nucl. Phys. **B228**, 301 (1983).

[41]A. Pinch and J. Bernabeu, Z. Phys. **C22**, 197 (1984).

[42]A. Bramon *et al.*, Phys. Lett. **B41**, 609 (1972); J. J. Sakurai, Phys. Lett. **B46**, 207 (1973); M. Greco, Nucl. Phys. **B63**, 398 (1973).

[43]M. Pratap and J. Smith, Phys. Rev. **D5**, 2020 (1972).

[44]L. Bergstrom and H. Snellman, Z. Phys. **C8**, 363 (1981).

[45]G. A. Kozlov *et al.*, Z. Phys. **C21**, 63 (1983); G. A. Kozlov *et al.*, Preprint E2-84-256, Joint Institute for Nuclear Research, Dubna, 1984.

[45]G. V. Efimov *et al.*, Pis'ma Zh. Eksp. Teor. Fiz. **32**, 60 (1980) [JETP Lett. **32**, 55 (1980)]; M. Dineĭkhan *et al.*, in: Trudy mezhdunarodnogo seminara po problemam vysokikh enegriĭ i kvantovoĭ teorii polya (Proceedings of the International Seminar on Problems of High Energies and Quantum Field Theory), Protvino, 1981, Vol. 1, p. 240; Preprint Nos. R2-81-131, R2-81-272, Joint Institute for Nuclear Research, Dubna, 1981.

[47]B. V.Martem'yanov, Yad. Fiz. **31**, 999 (1980) [Sov. J.Nucl. Phys. **31**, 515 (1980)].

[48]"Review of particle properties," Rev. Mod. Phys. **56**, 304 (1984).

[49]G. Kopp, Phys. Rev. **D10**, 932 (1974).

[50]V. L. Eletsky *et al.*, Phys. Lett. **B122**, 423 (1983).

[51]W. D. Apel *et al.*, Yad. Fiz. **30**, 366 (1979) [Sov. J. Nucl. Phys. **30**, 189 (1979)]; A. Weinstein *et al.*, Phys. Rev. **D28**, 2896 (1983); J. Olsson, Doklad na XX Mezhdunarodnoĭ konferentsii po fizike vysokikh energiĭ (Twentieth International Conference on High-energy Physics), Leipzig, 1984, B20/6/1.

[52]B. D. Hyams *et al.*, Phys. Lett. **B29**, 128 (1969).

[53]D. A. Geffen and B. L. Young, Phys. Lett. **B15**, 316 (1965).

[54]V. A.Viktorov *et al.*, Yad. Fiz. **32**, 1002 (1980) [Sov. J. Nucl. Phys. **32**, 518 (1980)]; Phys. Lett. **B97**, 471 (1980).

[55]S. D. Drell, Nuovo Cimento **11**, 693 (1959).

[56]S. Berman and D. Geffen, Nuovo Cimento **18**, 1192 (1960).

[57]L. Bergstrom, Z. Phys. **C14**, 129 (1982).

[58]G. B.Tupper and M. A. Samuel, Phys. Rev. **D26**, 3302 (1982).

[59]L. Bergstrom and E. Ma, Phys. Rev. **D29**, 1029 (1984).

[60]G. B. Tupper and M. A. Samuel, Phys. Rev. **D29**, 1031 (1984).

[61]M. D. Scadron and M. Visinescu, Phys. Rev. **D29**, 911 (1984).

[62]Ll. Ametller *et al.*, Phys. Rev. **D30**, 251 (1984).

[63]B. D. Hyams *et al.*, Phys. Lett. **B24**, 634 (1967).

[64]J. Fisher *et al.*, Phys. Lett. **B73**, 364 (1978).

[65]J. S. Frank, Phys. Rev. **D28**, 423 (1983).

[66]"Experiments at CERN in 1983," Preprint CERN, Geneva, 1983; N. W. Tanner, in: Particles and Nuclei: Tenth International Conference, Book of Abstracts, Vol. II, K3, Heidelberg, July 30-August 3, 1984.

[67]T. P. Cheng, Phys. Rev. **162**, 1734 (1967).

[68]J. Bernstein, G. Feinberg, and T. D. Lee, Phys. Rev. **139**, 1650 (1965).

[69]V. A. Viktorov *et al.*, Yad. Fiz. **33**, 1529 (1981) [Sov. J. Nucl. Phys. **33**, 822 (1981)]; Phys. Lett. **B105**, 239 (1981).

[70]J. Ellis *et al.*, Nucl. Phys. **B106**, 292 (1977).

[71]A. I. Vaĭnshteĭn *et al.*, Usp. Fiz. Nauk **131**, 537 (1980) [Sov. Phys. Usp.

23, 429 (1980)].
[72]A. S. Martynov *et al.*, Yad. Fiz. **23**, 93 (1976) [Sov. J. Nucl. Phys. **23**, 48 (1976)].
[73]M. R. Jane *et al.*, Phys. Lett. **B59**, 99 (1975).
[74]A. A. Wehmann *et al.*, Phys. Rev. Lett. **20**, 748 (1968).
[75]A. Rittenberg *et al.*, Phys. Rev. Lett. **15**, 556 (1965).
[76]A. Stetz *et al.*, TRIUMF Proposal 217, 1982; J. M. Poutisson, TRIUMF Preprint TRI-pp-83-93, 1983.
[77]J. W. Alcock *et al.*, Nucl. Phys. **B145**, 85 (1978); I. H. Dunbar, Phys. Rev. Lett. **41**, 210 (1978).
[78]S. Berger and B. Feld, Phys. Rev. **D8**, 3875 (1973); N. Levy *et al.*, Phys. Rev. **D13**, 2662 (1976).
[79]A. S. Carroll *et al.*, Phys. Rev. Lett. **44**, 525 (1980).
[80]L. Bergstrom *et al.*, Phys. Lett. **B131**, 229 (1983).
[81]R. E. Shrock and M. B. Voloshin, Phys. Lett. **B87**, 375 (1979); V.Barger *et al.*, Phys. Rev. **D25**, 1860 (1982); E. Ma and A. Pramudita, Phys. Rev. **D24**, 2476 (1981); L. Bergstrom *et al.*, Phys. Lett. **B134**, 373 (1984).
[82]S. Wolfram, Nucl. Phys. **B117**, 109 (1976); P. Hercseg and C. M. Hoffman, Phys. Lett. **B100**, 347 (1981); L. B. Okun, Preprint ITEP-149, Institute of Theoretical and Experimental Physics, Moscow, 1983.

Translated by Dave Parsons